

Sanfix

ERG Co  
ystems Division

R. R. Miley

NO.  
ASTIR-  
TM-37

REV. NO.

PAGE 1 OF

DATE Jan. 1974

## LSG FLIGHT CONFIGURATION

### SIMULATION

Prepared by

R. Wallace Jr.

R. Wallace

Approved by

D. Fithian

D. Fithian

### SUMMARY

The sensor beam of Flight LSG has been centered by partially uncaging the lunar masses. In this configuration the sensor exhibits a 1.5 Hertz oscillation. Attempts to duplicate this configuration employing the Qual LSG were unsuccessful. The beam of the Qual Model was centered employing both the mass change mechanism and the beam clamp mechanism, however, the characteristic oscillation for both conditions was approximately 17 Hertz. Calculations indicate a possible mechanism which would cause oscillation in the order to 1.5 Hertz would be a rocking motion of the lunar masses pivoted from one edge of the caging mechanism. Since the Qual instrument could not be configured to produce the 1.5 Hertz oscillation, data taken from the Flight LSG exercises performed on September 26, 1973 was used to develope the sensor transfer functions and also the response characteristics of the free modes output. Response curves for a 2 Hertz sensor with a Q of 25 and for a 1 Hertz sensor with a Q of 12.5 are presented in the attached appendix.

### INTRODUCTION

The Flight LSG lunar masses are approximately 0.5 grams too light and therefore the sensor beam cannot be centered between the capacitive plates in the normal fashion. Since it is necessary to center the beam to obtain free modes information, the Flight LSG beam has been centered by partially uncaging the mass cage assembly (reference Figure 1) which operates vertically; moving upward to uncage the masses and pan and downward to cage the masses and pan. In the masses caged position the mass cage assembly, which moves as a single structure, moves to its lowest position clamping the masses both at the top of the lunar masses and below via the lower caging springs. Because the lunar masses are too light, the masses (minor trim masses are not shown in Figure 1) are pulled by the LaCoste spring against the caging assembly when the caging assembly is partially uncaged. The beam is therefore suspended between the LaCoste spring and a small relatively stiff spring located between the beam and pan suspension wires. The Qual LSG can be used to simulate the spring tension of the Flight LSG by driving the coarse adjusting screw to its upper stop and by partially uncaging the lunar masses. In this configuration as shown in Figure 1, the lunar masses rest on the lower portion of the mass cage assembly because of the 6 times difference in gravity. The 0.5 gram

LSG Flight Configuration Simulation

NO.  
ASTIR-  
TM-37

REV. NO.

PAGE 3 OF \_\_\_\_\_  
DATE Jan. 1974

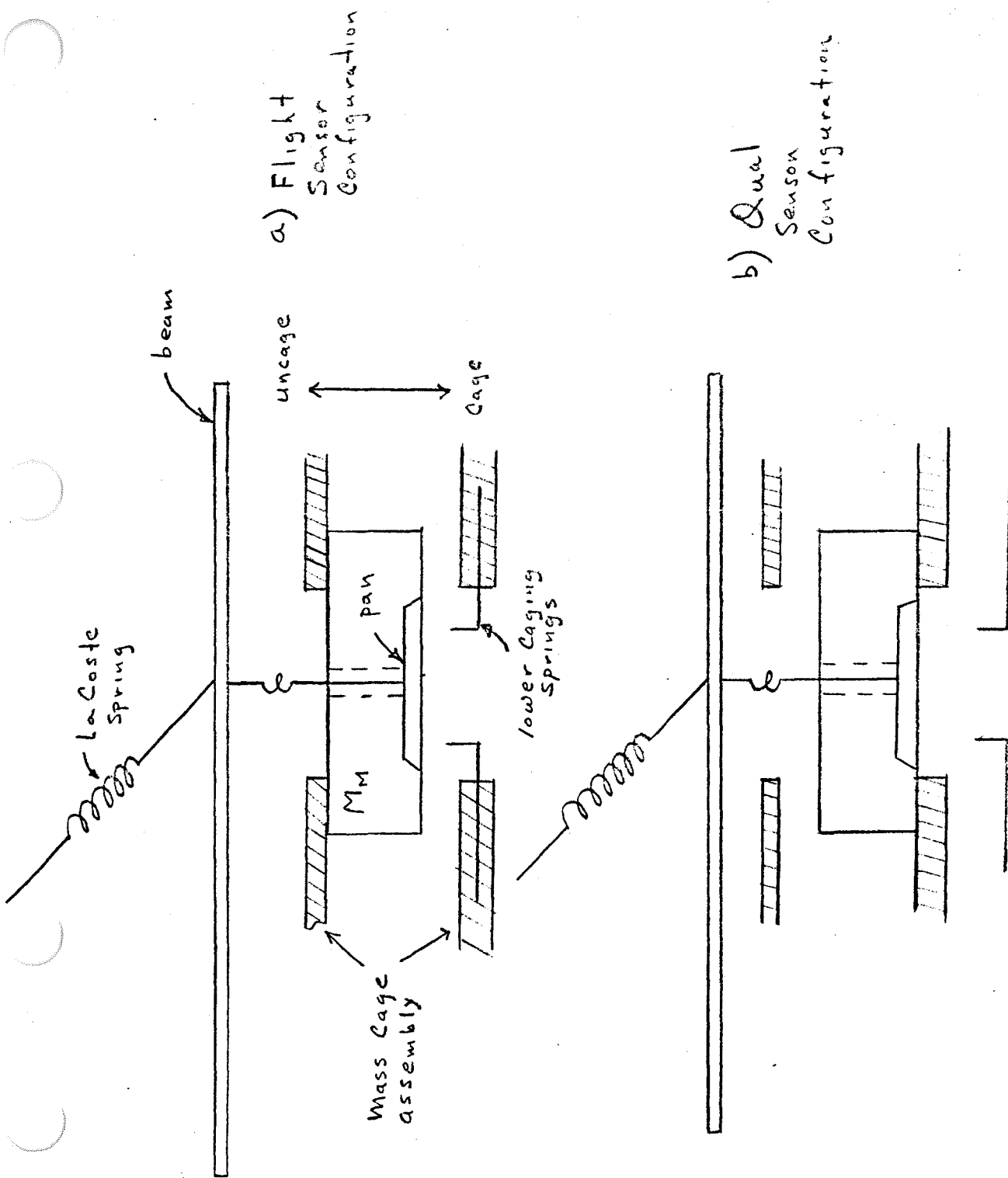


Figure 1 LSG Simplified Sensor Configurations



## LSG Flight Configuration Simulation

NO. ASTIR- REV. NO.  
TM-37

PAGE 4 OF \_\_\_\_\_

DATE Jan 1974

tension is provided by the coarse screw adjustment which has a total range equivalent to approximately 1 gram and is adjusted to operate at mid range on earth.

### TEST DESCRIPTION

The Qual LSG was operated in the normal PIA test setup employing the LSG ETS with the LSG at inversion temperature. An analog recorder monitored the tide, free modes and seismic channels. A baseline reading line measurement was taken with the coarse screw shaft encoder readout at 3126.410. The coarse screw was then driven toward the upper stop when difficulty with the screw drive similiar to that noted in December 1972 was noted. (During the Apollo 17 mission in December 1972 a cold start test was conducted on the qual instrument to simulate flight operation. During this test the screw drive did not rotate the correct number of revolutions per gross slew. This "sticky" coarse screw operation appeared to be similiar to a condition noted during qualification testing, only to a lesser extent, which cleared itself after operating the screw back and forth several times. The "sticky" condition was attributed to the oil lubrication used on the screws.) During the present test the screw was found to rotate 36 revolutions after 10 gross slews which is normally equivalent to 1030 revolutions. It was calculated that the number of revolutions required to drive the screw from the reading line position to the top stop was approximately 1532. A discussion was held with the sensor manufacturer and personnel at BxA relative to the mechanism causing this problem. It was the opinion of the sensor manufacturer that the screw threads were not damaged and because of the method employed to couple the screw drive to the shaft encoders it was concluded that the most probable mechanism which could cause this problem was oil on the screws which causes the drive motor to stall. Additional attempts were made to drive the screw but were unsuccessful.

Since the coarse screw position was above the reading line value, a positive tension, much less than that on the flight sensor, could be achieved by centering the beam with the mass cage assembly. A series of tests were run in this configuration to determine the beam's resonant behavior:

1. Beam centered, integrator normal with integrator saturated low and bias in/out commanded

*Lendir*

Aer. SCS  
Systems Division

LSG Flight Configuration Simulation

NO.  
ASTIR-  
TM-37

REV. NO.

PAGE 5 OF

DATE Jan. 1974

2. Same as 1 with integrator saturated high
3. Beam centered, integrator normal with bias in and with bias out and manual excitation (tap sensor).

The beam was then centered using the beam clamp mechanism. In this configuration, shown in Figure 2, the beam is allowed to travel to the upper beam stop by lifting all the lunar masses off of the pan (earth mass configuration). The beam is then centered by partially clamping the beam clamp mechanism which normally would clamp the beam against the lower beam stop. A similiar series of tests to those noted above were performed.

#### TEST RESULTS

The tests performed did not generate sensor oscillations in the order of 1.5 Hertz. Figures 3 thru 17 are typical seismic traces for the test conditions noted. In general, there was a 17 Hertz resonant oscillation present in all traces for all test conditions attempted. Electronic excitation using the bias in/out command to provide a coulomb force step input to the sensor beam gave inconsistant results. On one or two occasions a low frequency component subsequent to sending the bias commands was noted in the noise level, however, these results could not be duplicated with any consistancy and may have been a random low frequency noise component. The 17 Hertz oscillations was more predominant when the beam was centered using the beam clamp mechanism. The background seismic activity was reduced and the 17 Hertz oscillation appeared to be generated from a relatively high Q source. Since the beam motion at the front of the sensor is inhibited physically by the clamp mechanism it is assumed the 17 Hertz is caused by beam motion at the rear suspension of the sensor. The beam is suspended at the rear on each side by wire springs to provide a virtual frictionless pivot. During previous qual testing a high frequency seismic component in the order of 20 Hertz was noted during noise tests and this activity was determined to be caused by the rear suspension springs.

#### ANALYSIS

Since the results of the experiments with the qual LSG were negative, data taken from the Flight LSG operation of 26 September were used to determine the sensor transfer function for the flight sensor. The computations

LSG Flight Configuration Simulation

NO. ASTIR-TM-37 REV. NO.  
PAGE 6 OF \_\_\_\_\_  
DATE Jan. 1974

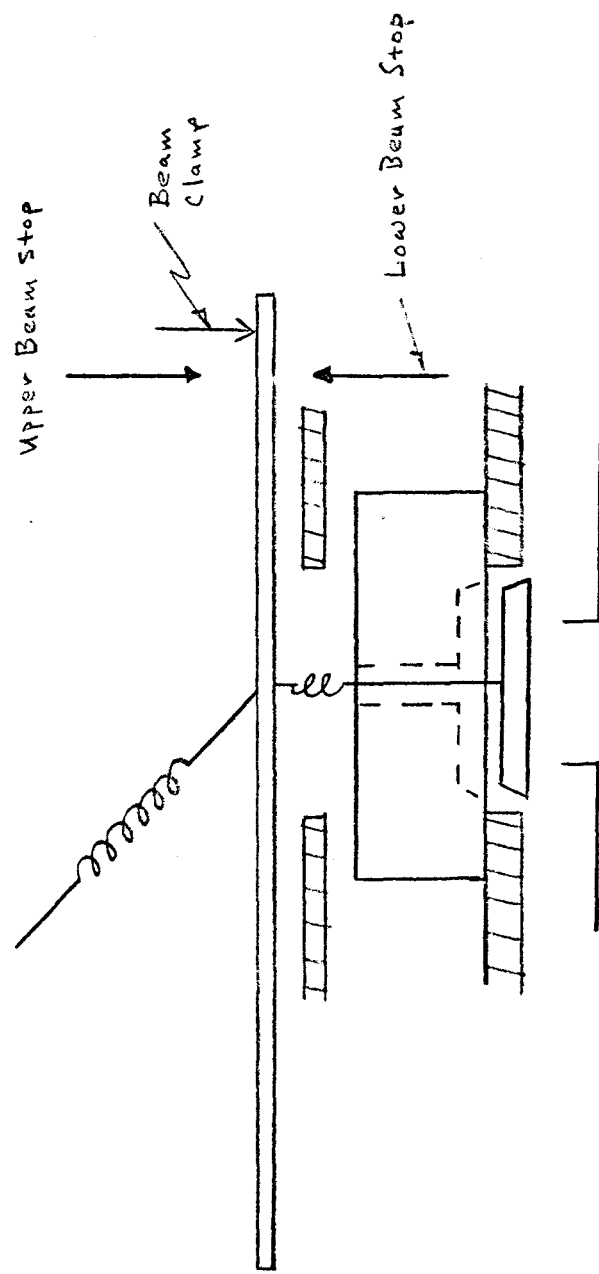


Figure 2 Qual LSG Centered via Beam Clamp



## LSG Flight Configuration Simulation

NO. ASTIR- REV. NO.  
TM-37  
PAGE 7 OF \_\_\_\_\_  
DATE Jan. 1974

and response curves are provided in Appendix A for a 2 Hertz sensor as determined on 26 September and for a 1 Hertz sensor. The 1 Hertz resonance is believed to be achievable by additional adjustments. Appendix B provides the Flight LSG coarse and fine screw conversion factors along with the sensitivity calculations used to determine the resonant frequency of the sensor in the partially uncaged condition. These calculations used the relationship

$$W = g / X$$

where  $W = 2 f$

$g$  = the change in the coarse screw adjustment in gals.

$X$  = displacement of the sensor beam c. g. in cm.

Also included in Appendix B is a summary of the flight beam behavior during the September 26 tests.

ndix  
rosce  
ystems Division

LSG Flight Configuration Simulation

NO. ASTIR- TM-37	REV. NO.
PAGE <u>8</u>	OF _____
DATE Jan. 1974	

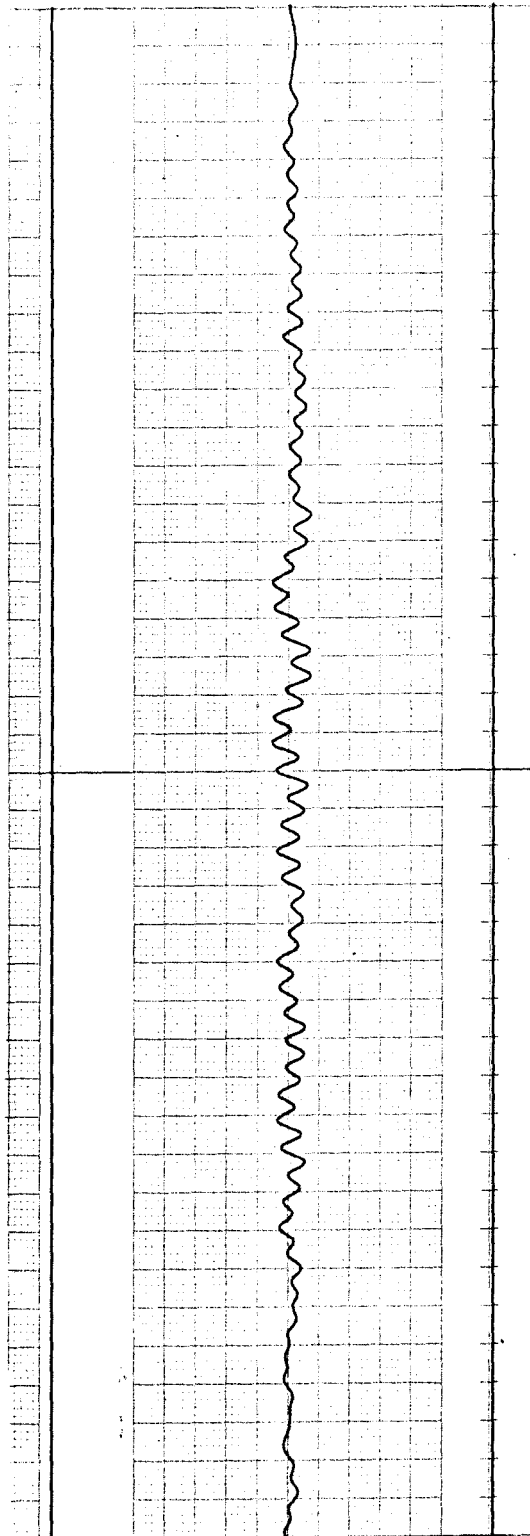


Figure 3 16.8 Hz Noise Signal with Beam Centered via MC.  
High Gain, PA = 1; 60 mm/sec, 0.1 volts/div.;  
Integrator Closed Loop and Saturated FS low,  
Bias in.

endix A

aerospace  
systems Division

LSG Flight Configuration Simulation

NO.  
ASTIR-  
TM-37

REV. NO.

PAGE 9 OF \_\_\_\_\_

DATE Jan. 1974

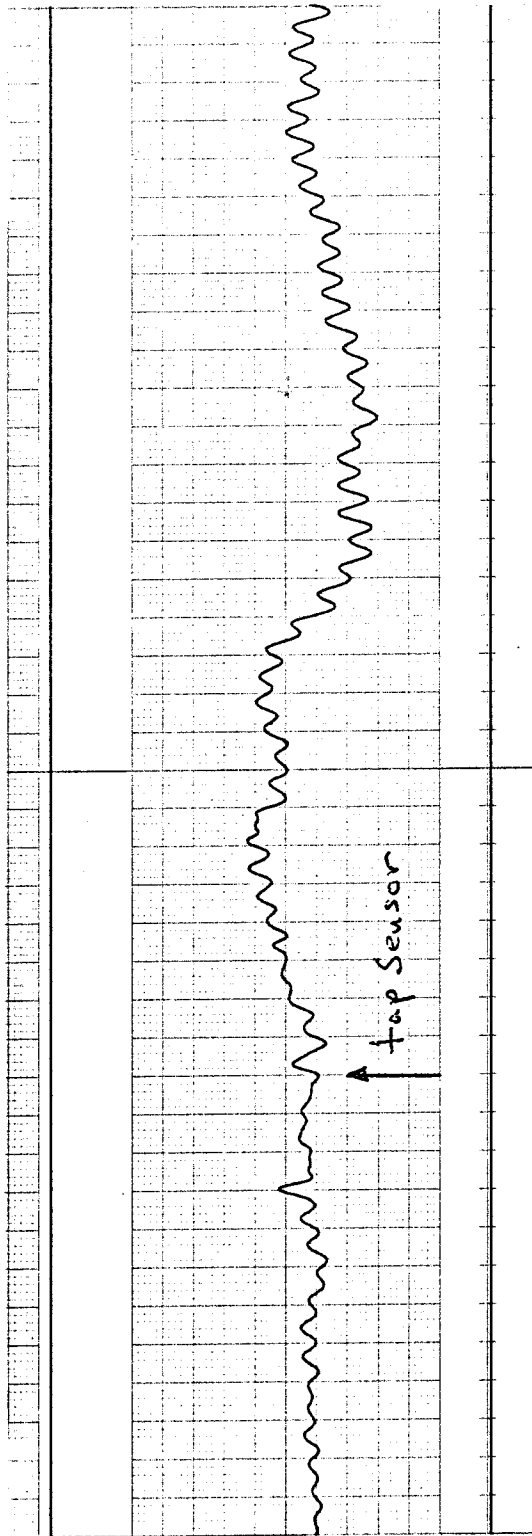


Figure 4 Manual Tap Sensor with Beam Centered via MC.  
High Gain, PA = 1; 60 mm/sec; 0.1 volts/div.;  
Integrator Closed Loop.



**Irospacé**  
**Structures Division**

LSG Flight Configuration Simulation

PAGE 10 OF \_\_\_\_\_  
DATE Jan. 1974

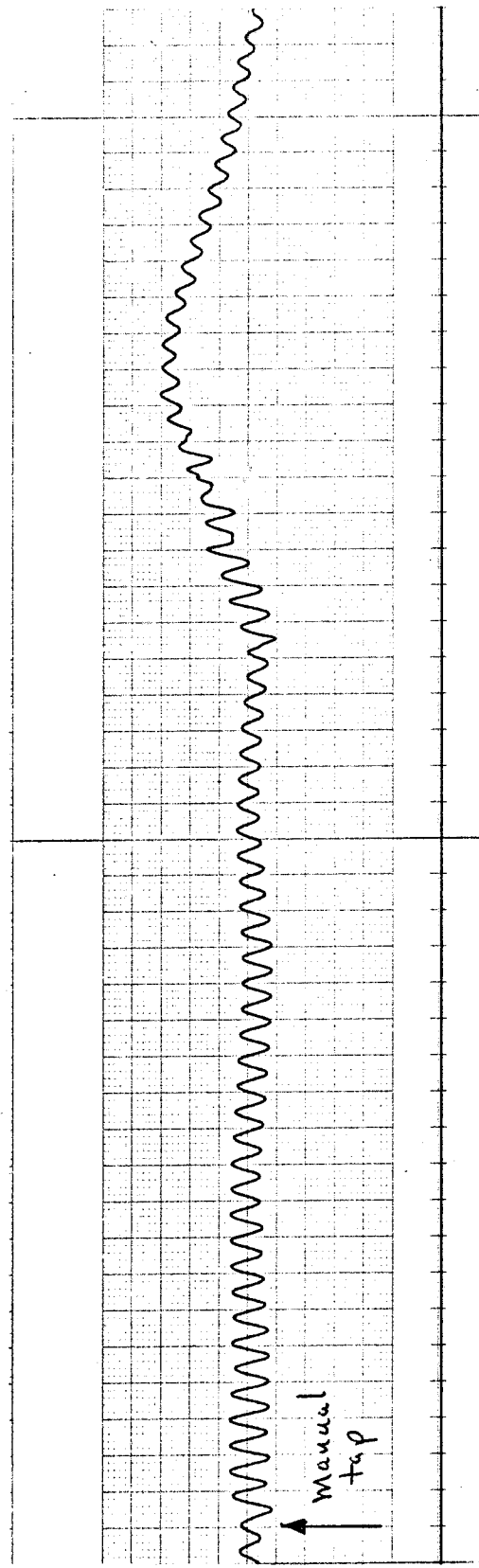


Figure 5 Manual Tap Sensor with Beam Recentered  
via MC. Some Conditions as Figure 4



**McDonnell  
Douglas  
Aerospace  
Systems Division**

**LSG Flight Configuration Simulation**

TM - 37

PAGE 11 OF \_\_\_\_\_

DATE Jan. 1974

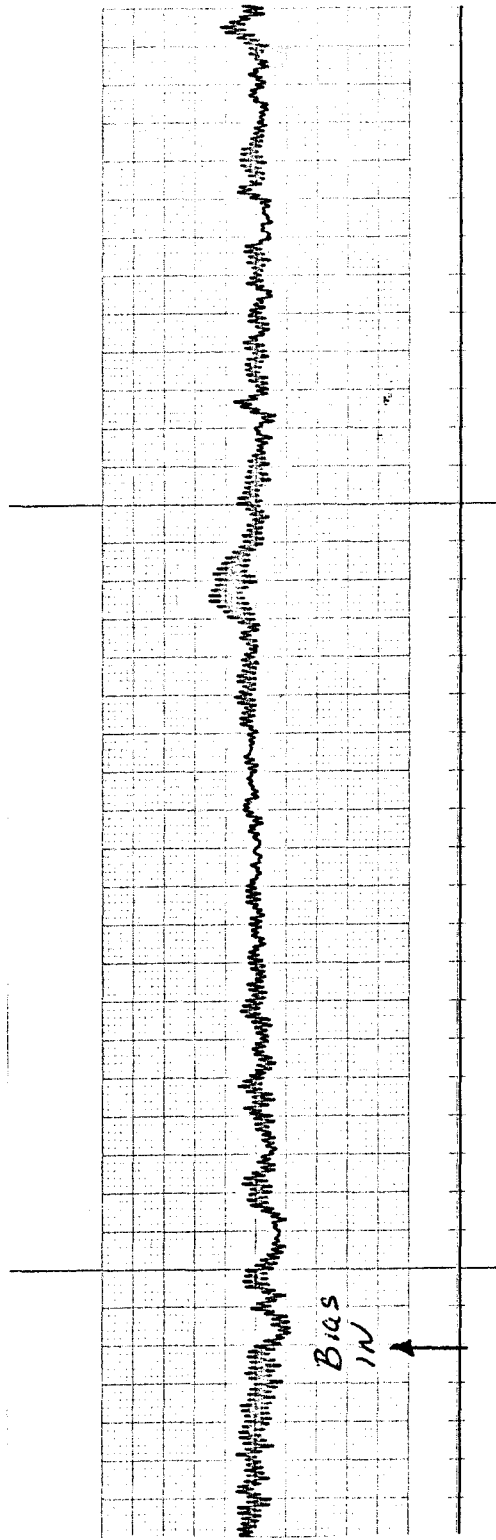


**Figure 6** Bias in Response with Beam Centered via MC.  
High Gain, PA = 1; 12 mm/sec. 0.1 volts/div;  
Integrator Closed Loop and Saturated FS High.

**rospace**  
**ste Division**

LSG Flight Configuration Simulation

PAGE 12 OF \_\_\_\_\_

DATE Jan. 1974

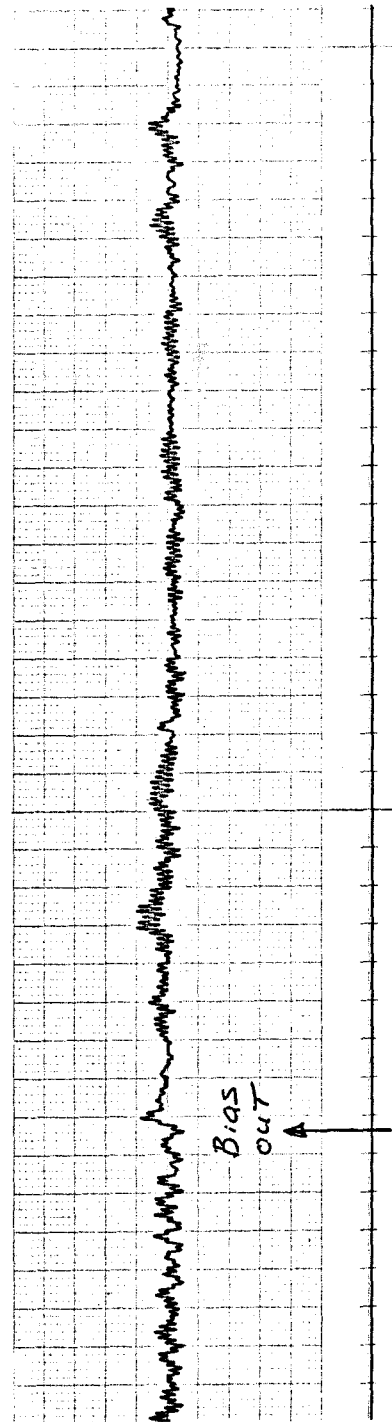


Figure 7 Bias Out Response with Beam Centered via MC.  
Same Conditions as Figure 6

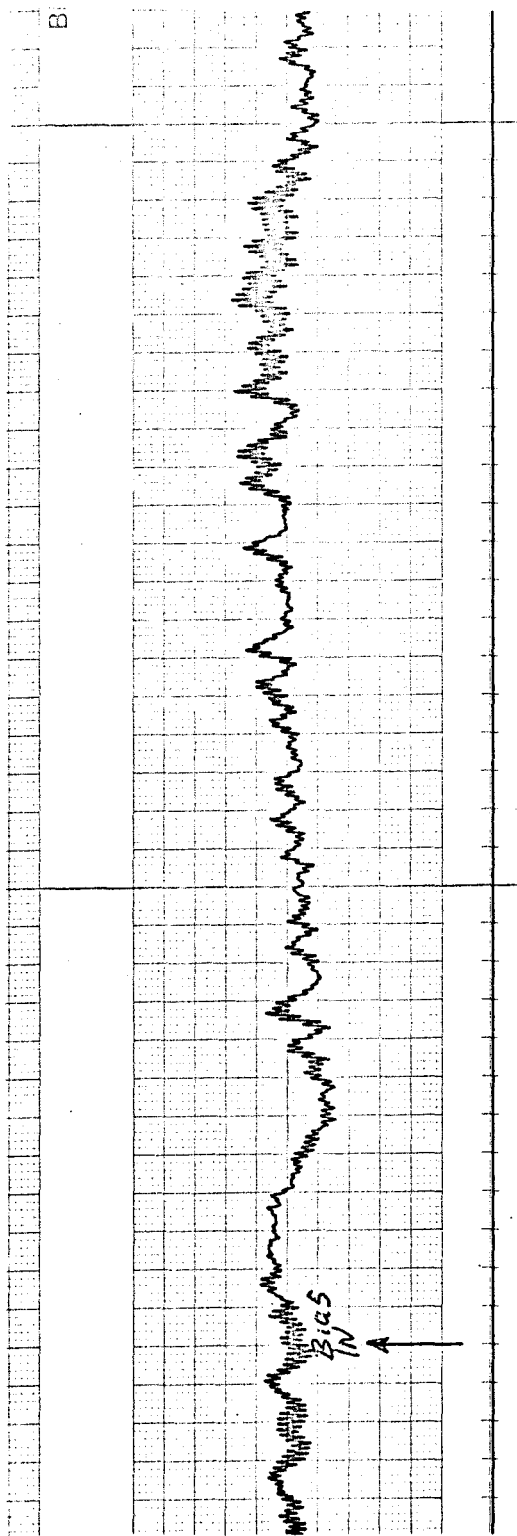
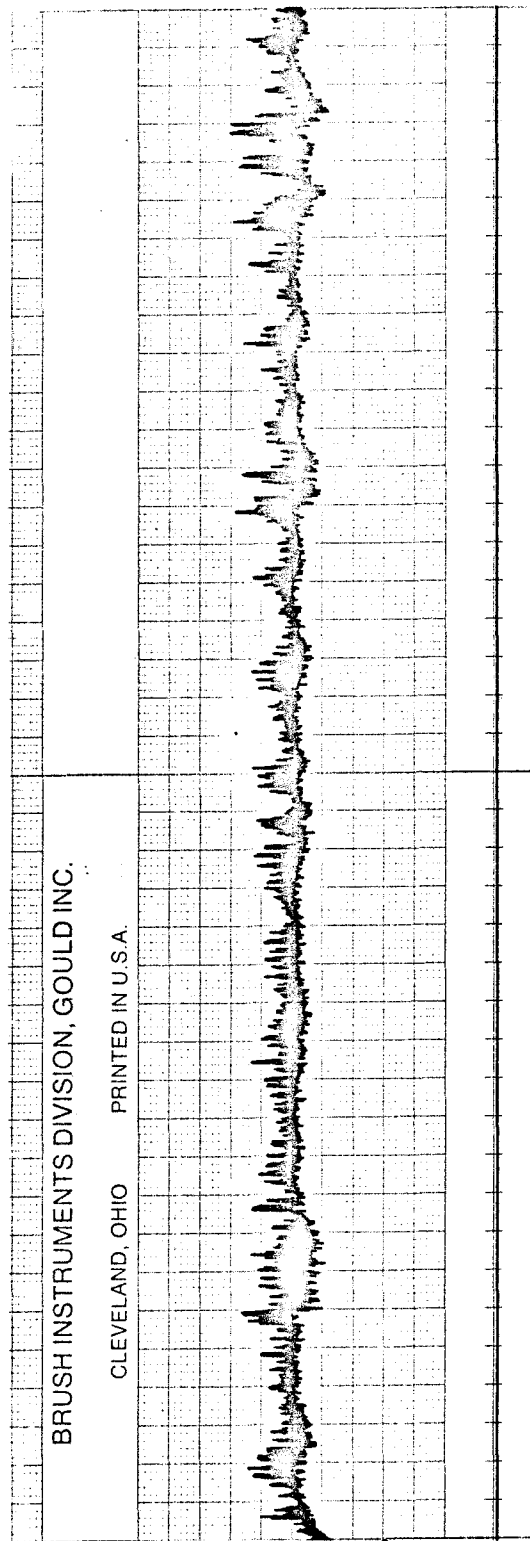


Figure 8 Bias in Response with Beam Centered via MC  
Same Conditions as Figure 6

ndix  
rospace  
ystems Division

LSG Flight Configuration Simulation

NO. ASTIR-  
TM-37 REV. NO.  
PAGE 14 OF \_\_\_\_\_  
DATE Jan. 1974



BRUSH INSTRUMENTS DIVISION, GOULD INC.

CLEVELAND, OHIO PRINTED IN U.S.A.

Figure 9 Unidirectional Seismic Noise with Beam Centered via MC.  
High Gain, PA = 1; 60 mm/minute, 0.1 volts/div.;  
Integrator Closed Loop, Bias Out

Bendix

Aerospace  
Systems Division

LSG Flight Configuration Simulation

NO.  
ASTIR-  
TM-37  
REV. N

PAGE 15 OF

DATE Jan. 1974

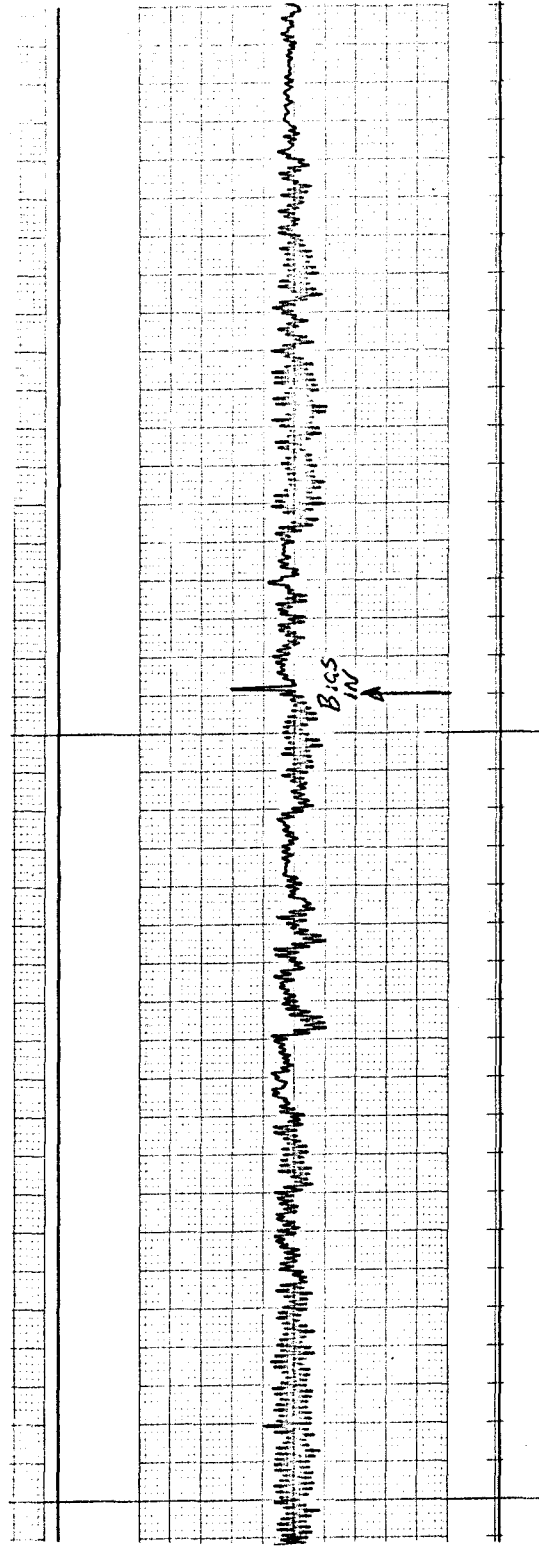


Figure 10 Bias In Response with Beam Centered via MC. High Gain, PA = 1; 12 mm/sec, 0.1 volts/div.; Integrator Closed Loop and Saturated Low



Aerospace  
Systems Division

LSG Flight Configuration Simulation

TM-37

PAGE 16 OF

DATE Jan. 1974

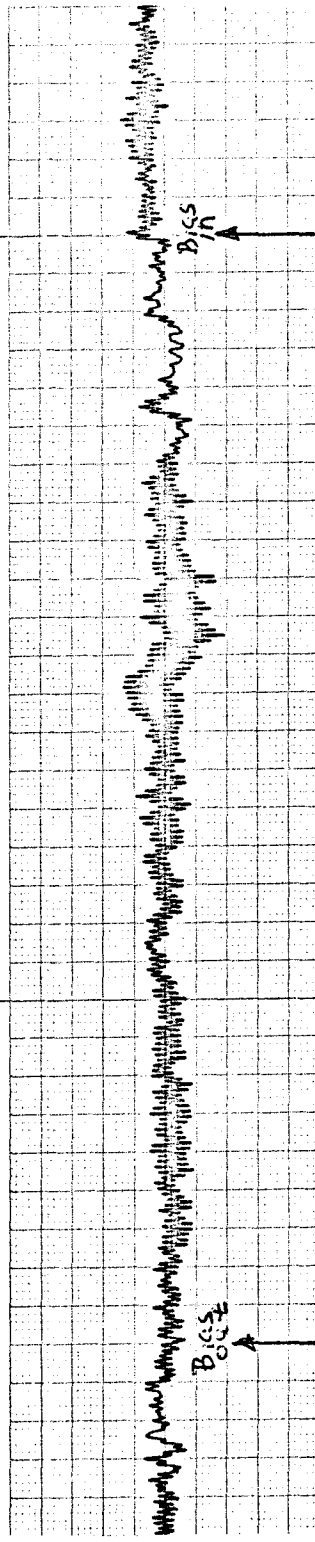
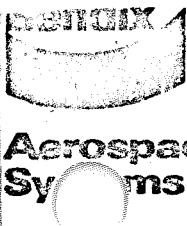


Figure 11 Bias Out/In Response Same Conditions as Figure 10



LSG Flight Configuration Simulation

TM-37

PAGE 17 OF       

DATE Jan. 1974

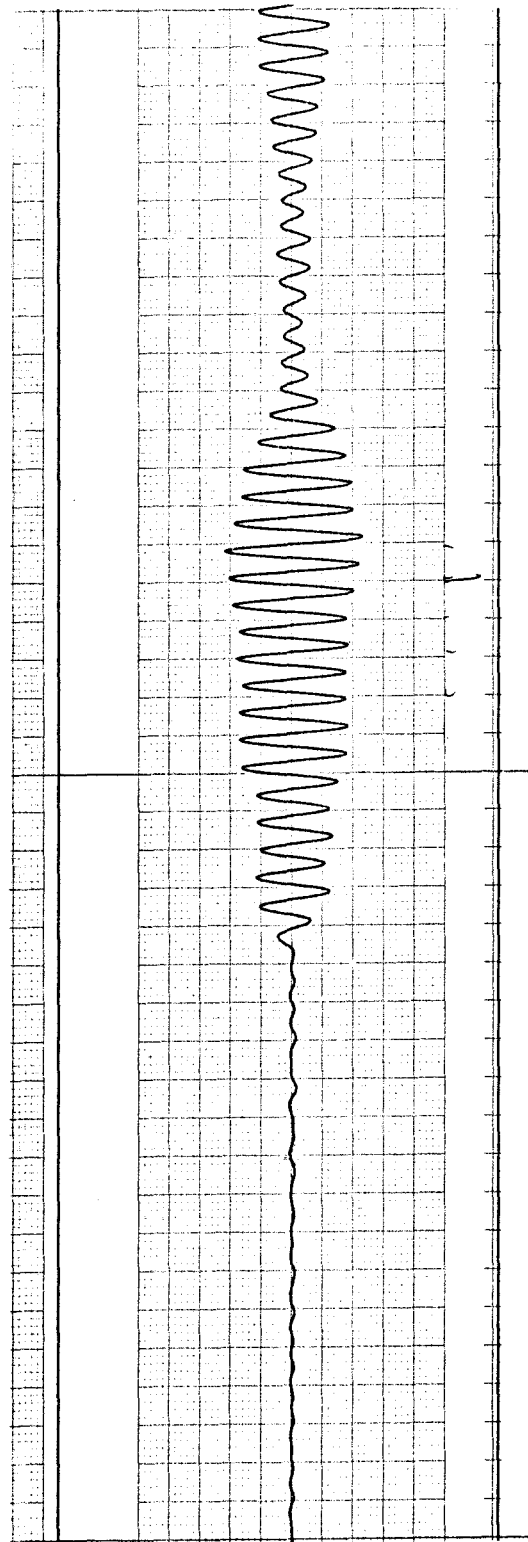


Figure 12 Seismic Noise Beam Centered via Beam Clamp Mechanism. High Gain, PA = 1; 60 mm/sec.  
0.1 volts/div.; Integrator Closed Loop Saturated  
Low, Bias In

**Aerospace  
Systems Division**

LSG Flight Configuration Simulation

PAGE 18 OF     
DATE Jan. 1974

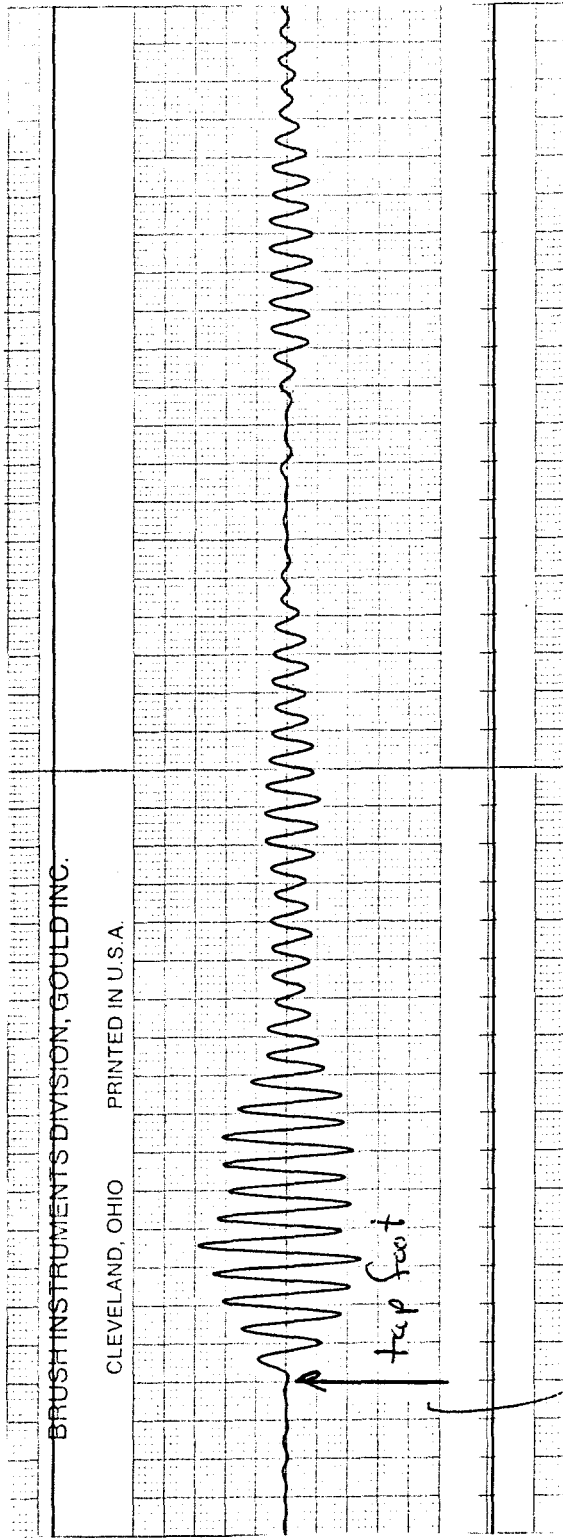


Figure 13 Manual Input (Tap Foot) Same Conditions as Figure 12

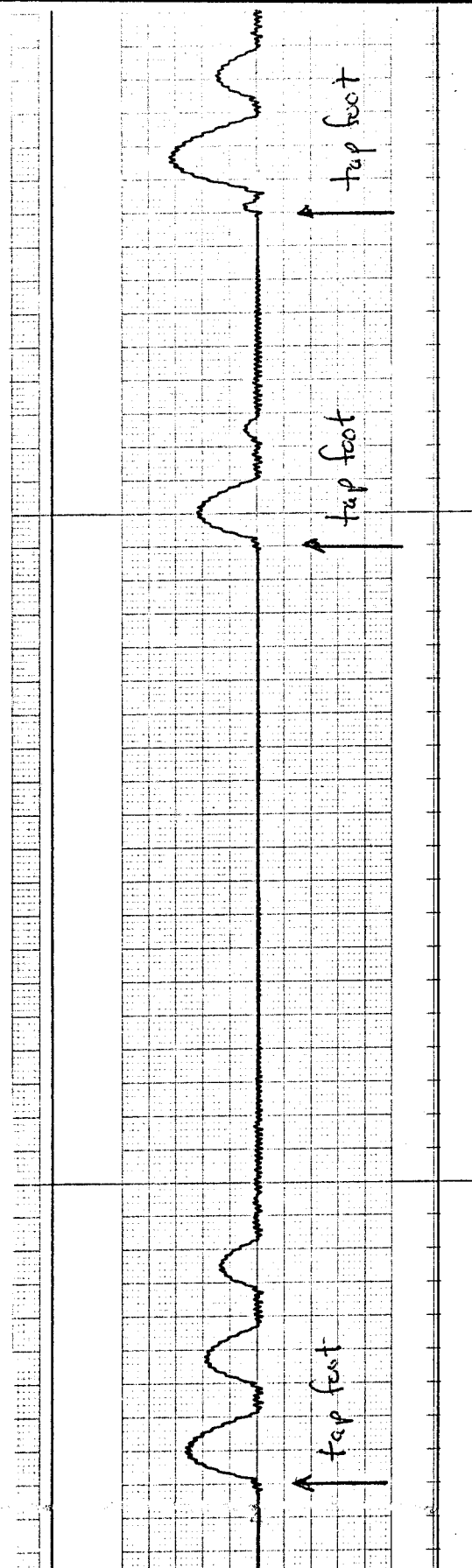


Figure 14 Manual Input (Tap Foot) Beam Centered via Beam Clamp Mechanism. Low Gain PA = 4; 12 mm/sec. 0.1 volts/div.; Integrator Closed Loop Saturated Low Bias In.



Bendix  
A space  
Systems Division

LSG Flight Configuration Simulation

NO. ASTIR-  
TM-37 REV. N  
PAGE 20 OF  
DATE Jan. 1974

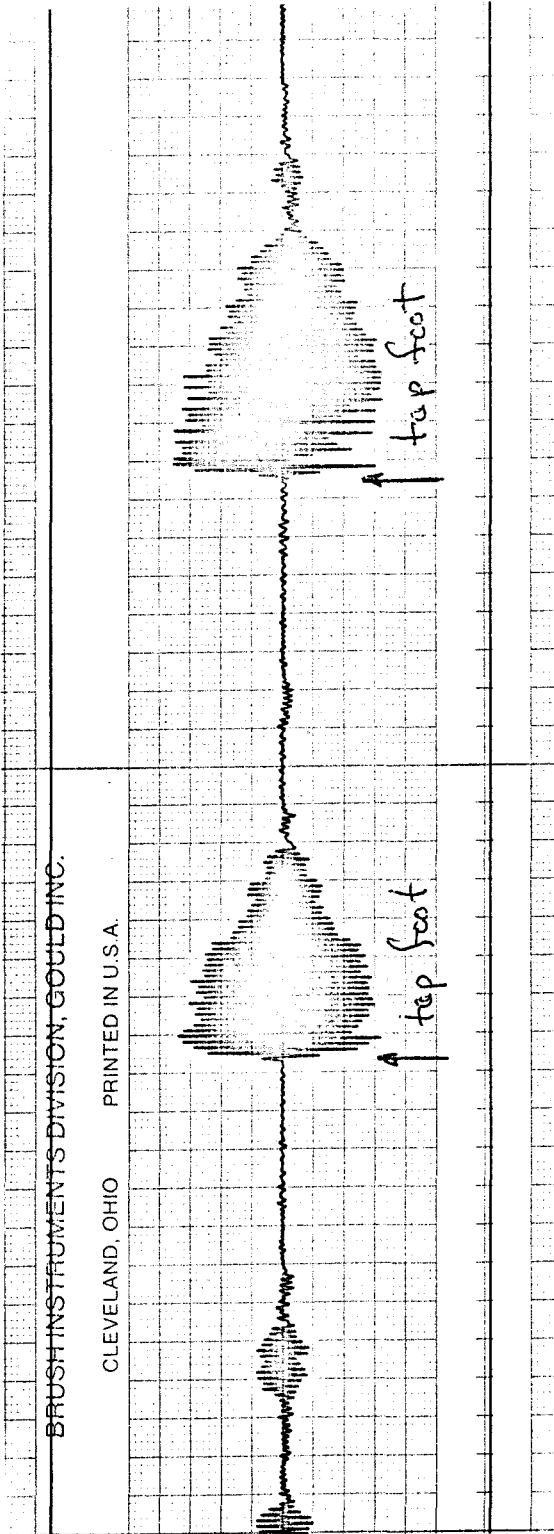


Figure 15 Manual Input (Tap Foot) Beam Centered via Beam Clamp Mechanism. High Gain PA = 1; 12 mm/sec. 0.1 volts/div.; Integrator Closed Loop Saturated Low Bias Out.



Aerospace  
Systems Division

LSG Flight Configuration Simulation

NO.  
ASTIR-  
TM-37

REV. NO.

PAGE 21 OF 1

DATE Jan. 1974

BUSH INSTRUMENTS DIVISION, GOULD INC.

CLEVELAND, OHIO PRINTED IN U.S.A.

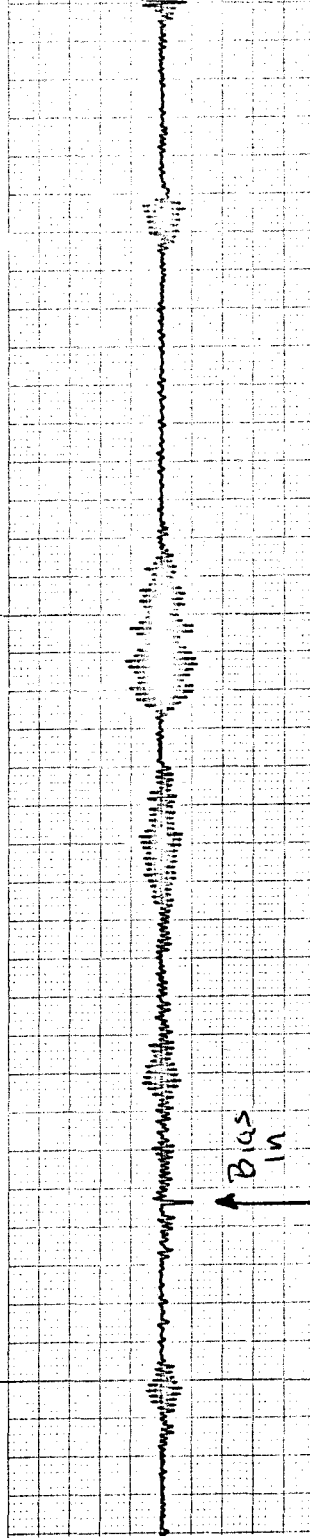


Figure 16 Bias In Response with Beam Centered via Beam Clamp Mechanism. Same Conditions as Figure 15.



Aerospace  
Systems Division

LSG Flight Configuration Simulation

NO.  
ASTIR-  
TM-37

REV. N

PAGE 22 OF   

DATE Jan. 1974

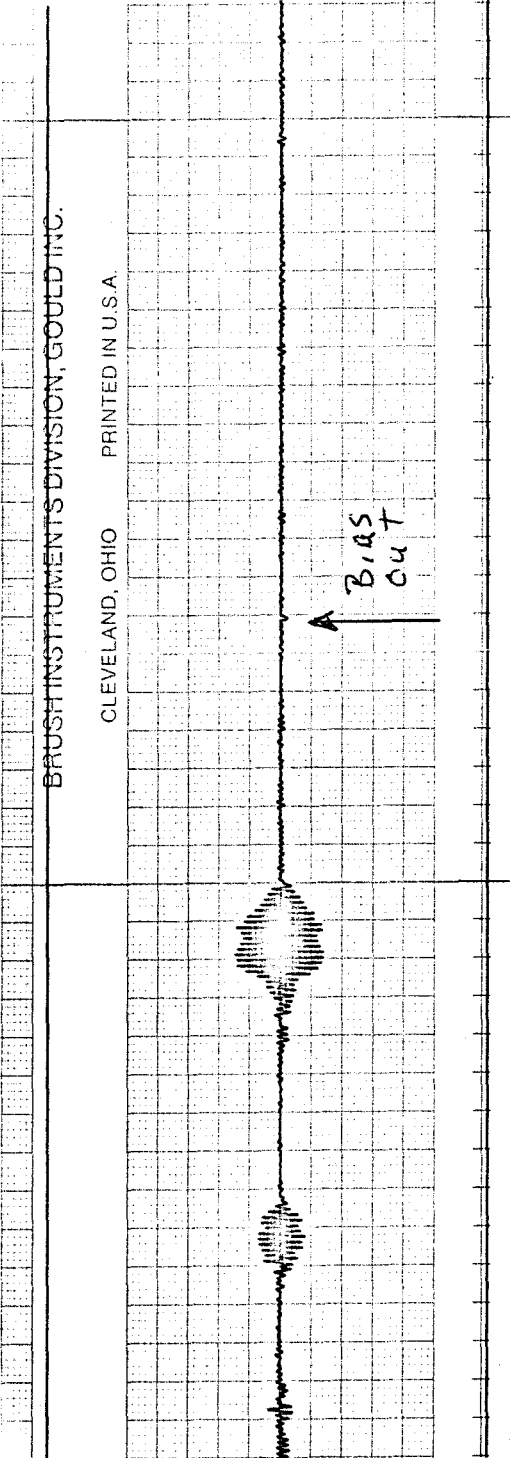


Figure 17 BIAS Out Response with Beam Centered via Beam Clamp Mechanism, Same Conditions as Figure 15.

endix  
Space  
ystems Division

NO.	REV. NO.
PAGE _____ OF _____	
DATE	

## APPENDIX A

### LSG Transfer Functions

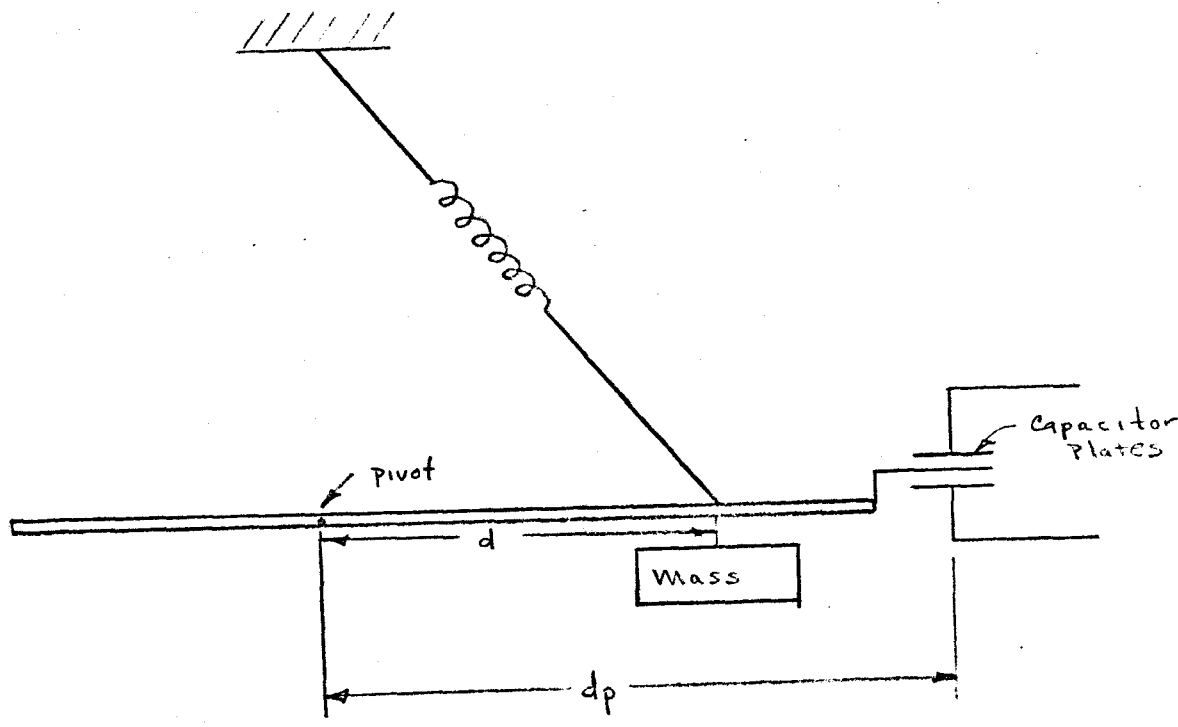


Figure 1 LSG Sensor

Equation of Motion

$$(1) \ddot{\delta} + 2 \xi \omega_0 \dot{\delta} + \omega_0^2 \delta = md \Delta g - dp F_e$$

which may be simplified to

$$(2) \ddot{x} + 2 \xi \omega_0 \dot{x} + \omega_0^2 x = \left(\frac{d}{dg}\right)^2 \Delta g - \left(\frac{d}{dg}\right)^2 \left(\frac{dp}{d}\right) \frac{F_e}{m}$$

where  $I = mdg^2$  and  $dg =$  radius of gyration around pivot.

$d$  = distance from pivot to c. g.

$F_e$  = capacitor plate electrical feed back force

---

\* Reference BxA Memo 984-683 of 19 May 1972 by M. Dela Cruz, entitled "Flight LSG Characteristics"

$x$  = c. g. vertical motion

$\omega_0$  = natural frequency of sensor

$m$  = total sensor mass

The electrical force on the beam is:

$$(3) \quad F_e = \frac{2 C_o V_o}{d_o} V_f - \frac{C_o}{d_o^2} \left[ (1 - k_s \cos \phi) V_c^2 + 2 V_o^2 + V_f^2 \right] X$$

where  $C_o = 3.5 \times 10^{-12}$  farads, the center plate to fixed plate capacitance

$d_o = .515 \times 10^{-1}$  cm, the center plate to fixed plate spacing

$V_o = 6.5V$ , the dc bias voltage plate to ground

$V_f = 0$  to  $5.5V$  (approximately), the feed back voltage

$k_s \approx \frac{2 C_o}{C_s + 2 C_o}$ , where  $k_s$  is the capacitance bridge constant

$C_s \approx 27-30 \times 10^{-12}$  farads, the stray capacitance of the sensor to preamp input including cable capacitance

$\phi = \tan^{-1} B/A$ , the bridge circuit phase angle

$B = \frac{1 - \alpha^2}{2 R_1 C_o W_c}, \quad \alpha = \frac{x}{d_o}$

$A = \frac{1 + (1 - \alpha^2)}{2 C_o} C_s$

$R_L = 5$  megohm, the load resistance seen by the bridge circuit

$W_c = 2\pi f_c$ , where the carrier frequency is  $3.3$  kHz

$V_c = 0.5V$ , the peak value of the carrier signal

From equation (2) and (3), the  $X$  terms may be combined to provide

## LSG Transfer Functions

PAGE A-3 OF \_\_\_\_\_

DATE Jan. 1974

$$(4) \ddot{x} + 2\zeta\omega_0 \dot{x} + \left\{ \omega_0^2 - \left( \frac{d}{dg} \right)^2 \left( \frac{dp}{d} \right) \left( \frac{1}{m} \right) \frac{C_o}{d} \zeta_o^2 \left[ (1 - ks \cos \phi) V_c^2 + 2V_o^2 + V_f^2 \right] \right\} x \\ = \left( \frac{d}{dg} \right)^2 \Delta g - \left( \frac{d}{dg} \right)^2 \left( \frac{dp}{d} \right) \left( \frac{1}{m} \right) \left( \frac{2 C_o V_o}{d_o} \right) V_f$$

Equation (4) is the system dynamics equation for closed loop operation. The block diagram for the system is shown in Figure 2, where the  $\omega_o^2$  term is the period of the sensor modified by the feedback electrostatic force shown in (4). In the closed loop configuration the two switches are thrown in the direction indicated. For open loop operation the switches are switched to the opposite direction and, since no electrostatic feedback force is present, the sensor transfer function becomes

$$(5) \frac{1}{s^2 + 2\zeta\omega_0 s + \omega_0^2}$$

where  $\omega_0$  is the natural period of the sensor and  $\zeta$  the damping factor.

Referring to Figure 2 the constants and transfer functions are:

$K_b = 88.4$  volts/cm, where  $K_b$  is the capacitance bridge transfer function and 88.4 V/cm is the measured value for the flight LSG.

Post Amp = 1-90, where the post amplifier gain may be stepped in 15 increments of 6 i.e. the 8th step is a gain of 48 (47.5 measured for flight).

Demodulator = 0.636, for the LSG demodulator transfer function

integrator =  $\frac{0.019}{s}$  for the ideal case and is

$$\frac{0.019}{s + 9.2 \times 10^{-6}} \text{ for the flight model}$$

where  $9.2 \times 10^{-6}$  is due to leakage and is the worst case value equivalent to 25 millivolts leakage in 5 minutes at 9 volts.

$$\left(\frac{d}{dg}\right)^2 \left(\frac{2 C_0 V_0}{d o m}\right) \frac{dp}{d} = 9.2 \times 10^{-5} \frac{\text{cm}}{\text{sec}^2 - \text{volt}}$$

factor, where the constants are as defined above and

$d$  = 3.06 cm and is the distance from pivot to c. g.

$dp$  = 4.53 cm and is the distance from pivot to the center of the capacitor plates

$dg$  = 1.03  $d$ , and is the radius of gyration

$m$  = .13375 kgram and is the flight sensor mass

There are four sensor cases which response curves are to be developed and they are:

- 1) Flight design open loop where the period of the sensor is 20.7 sec (lunar period), the damping factor is 0.755 (lunar)
- 2) Flight design closed loop where the period and damping factor are as 1) above but the transfer function is modified by the electrostatic feedback force
- 3) Flight sensor in the present configuration open loop where the period is 0.5 seconds and the Q of the sensor is 25.
- 4) Flight sensor in the present configuration closed loop where the period and Q of the sensor are as 3) above.

The transfer function for the four cases are

$$1) \quad \frac{1}{s^2 + 0.458 s + .0919}$$

$$2) \quad \frac{1}{s^2 + 0.458 s + .0719}$$

$$3) \quad \frac{1}{s^2 + 0.502 s + 158}$$

Appendix A

LSG Transfer Functions

NO.  
ASTIR-  
TM-37

REV. NO.

PAGE A-5 OF \_\_\_\_\_

DATE Jan. 1974

4)  $\frac{1}{s^2 + 0.502 s + 157.98}$

Referring to Figure 2, the free modes output is amplified and filtered by an amplifier with the following characteristics:

Gain 498

2-pole high pass .00083 Hz

butterworth filter

Phase lag filter 0.14 Hz and 70 Hz

the transfer functions for this element of the system is

$$\frac{1.9 \times 10^5 s^2}{(s^2 + 7.35 \times 10^{-3} s + 2.71 \times 10^{-5})(s + .88)(s + 440)}$$

Combining the filter transfer function with the appropriate open and closed loop sensor configuration described above and the remaining elements of the system shown in Figure 2, the transfer functions for the four cases are:

1)  $\frac{7.68 \times 10^8 s^2}{s^6 + 441.4 s^5 + 592.3 s^4 + 222.3 s^3 + 37.17 s^2 - 266 s + .000962}$

2)  $\frac{9.76 \times 10^6 s^2}{s^7 + 441.4 s^6 + 604.3 s^5 + 220.8 s^4 + 31.72 s^3 + 2.04 s^2 + .0141 s + .000049}$

3)  $\frac{7.68 \times 10^8 s^2}{s^6 + 440.9 s^5 + 769.7 s^4 + 69,6985 s^3 + 61,700 s^2 + 450 s + 1.65}$

4)  $\frac{9.76 \times 10^6 s^2}{s^7 + 441.4 s^6 + 769.7 s^5 + 69,769 s^4 + 61,703 s^3 + 451.8 s^2 + 1.668 s + .000049}$



Aerospace  
Systems Division

## Appendix A

### LSG Transfer Functions

NO.  
ASTIR-  
TM-37

REV. NO.

PAGE A-6 OF   

DATE Jan. 1974

Where the output of the functions are in units of volts/gal and the value of post amp gain was 47.5 (8th step). Figures 3 and 4 are plots of the response curves using the above functions. Figure 4 shows the response to the LSG if the period of sensor could be increased to 1 sec where the damping was assumed constant ( $Q = 12.5$ ).

## LSG Transfer Functions

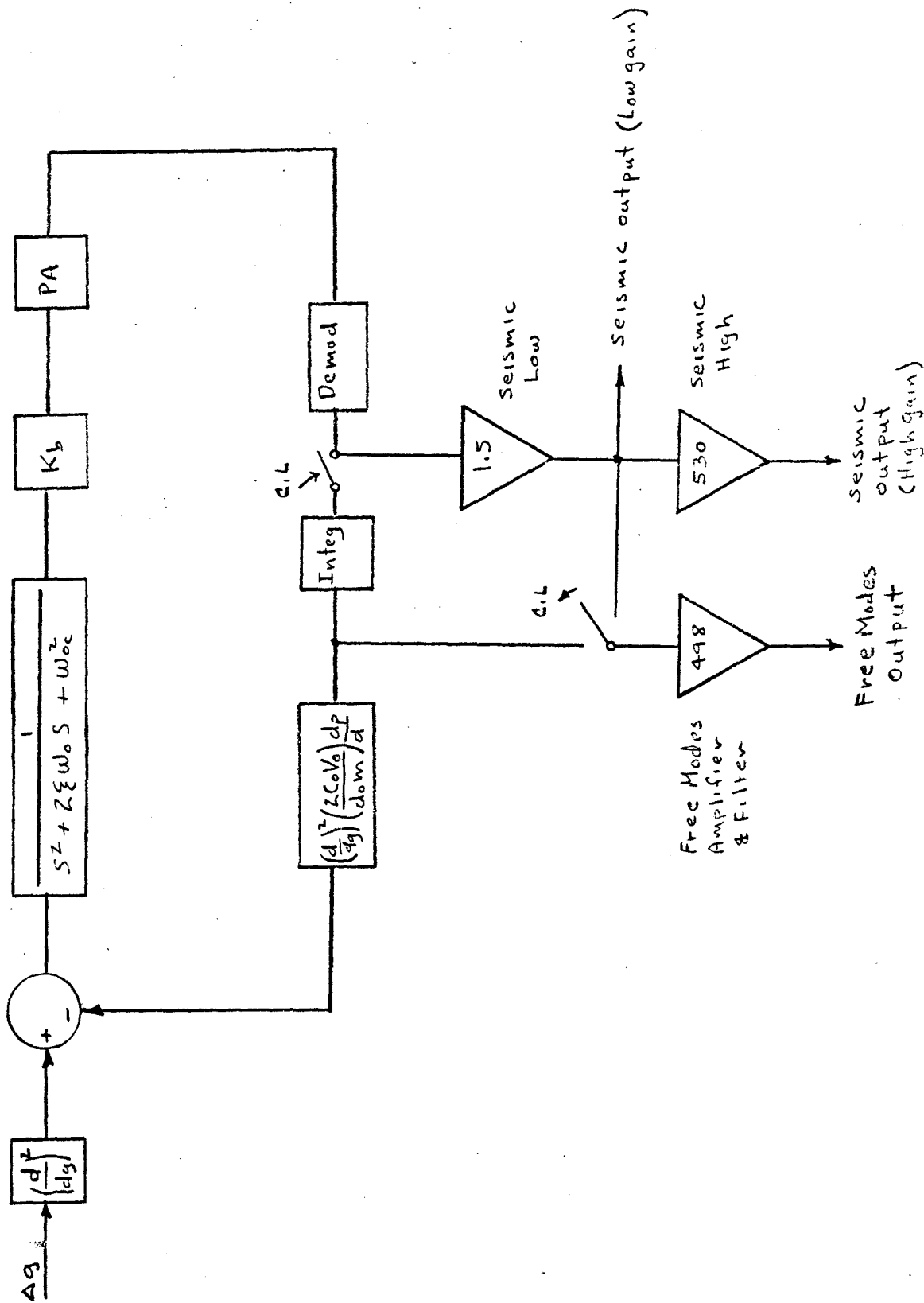
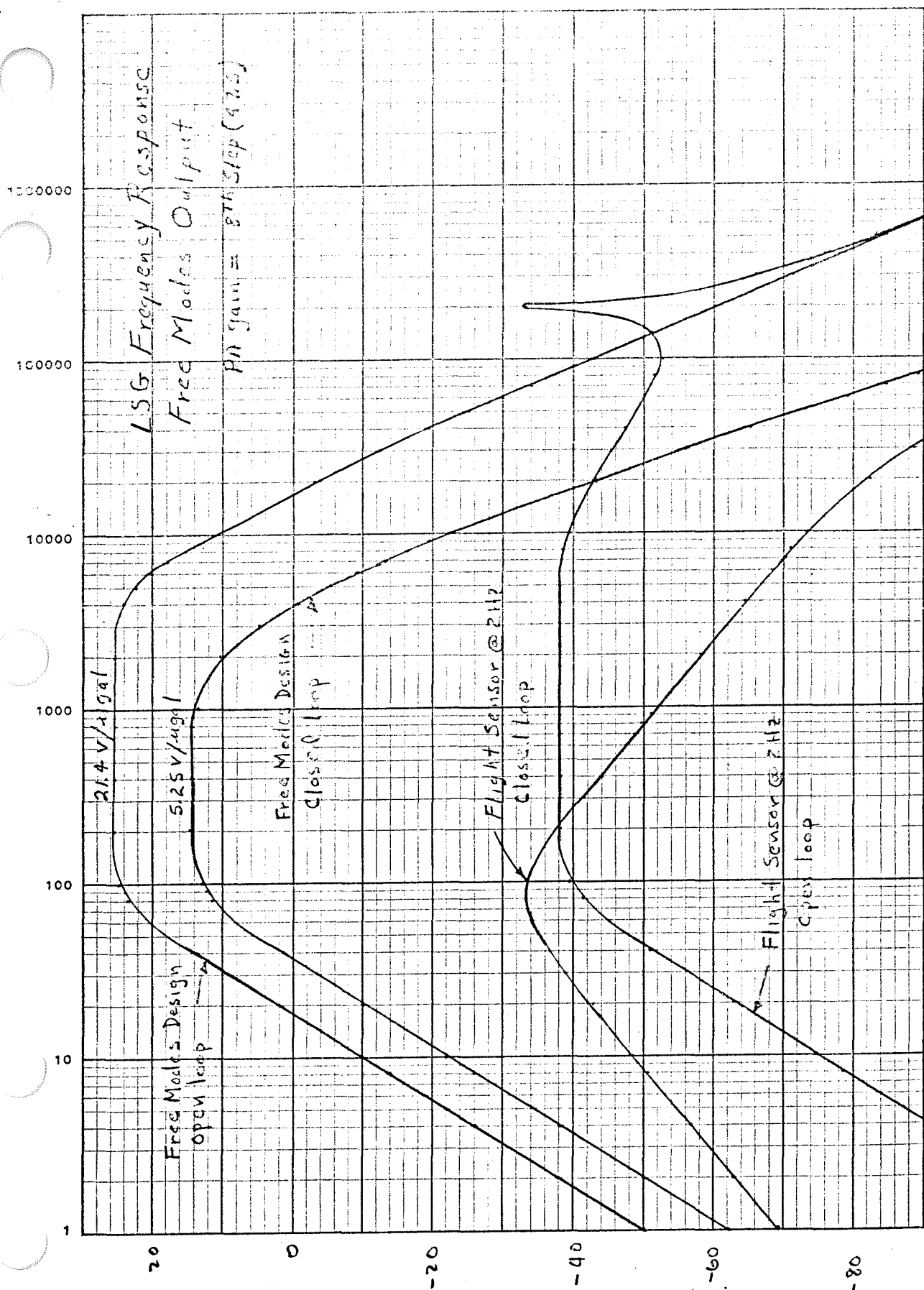
PAGE A-7 OF \_\_\_\_\_  
DATE Jan. 1974

Figure 2

Jan. 1974

MODEL

DATE

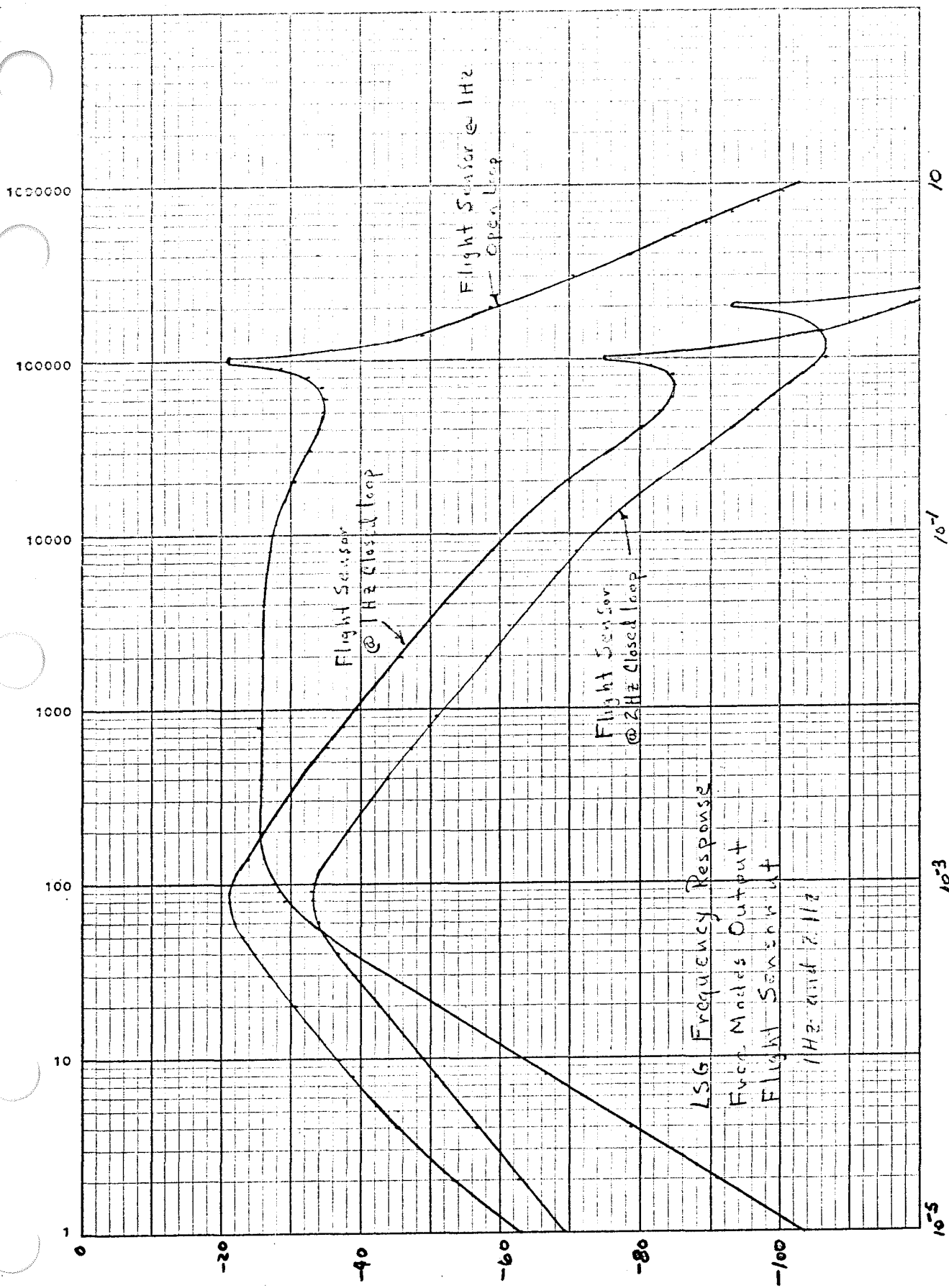


(10<sup>6</sup> m/V) 10<sup>6</sup> N/s + 10<sup>6</sup> N qd relative to vehicle

Fig. 3

MODEL

DATE

(10<sup>5</sup>m/s)(10<sup>5</sup>N/m<sup>2</sup>)

Frequency (Hz)

FIG. 4



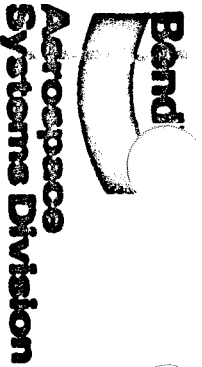
aerospace  
systems Division

PAGE \_\_\_\_\_ OF \_\_\_\_\_

DATE

## APPENDIX B

### LSG Sensitivity Calculations



## LSC Sensitivity Calculations

### Appendix B

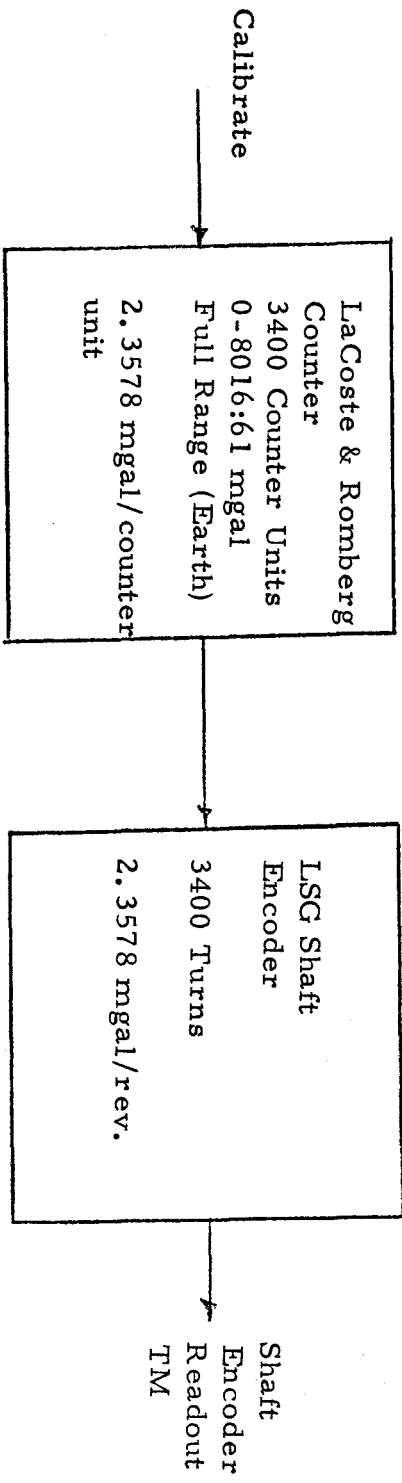
Mo.ASTIR- | REF. NO.

TM-37

PAGE B-1

OF

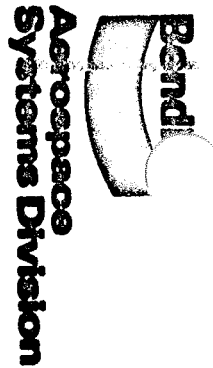
DATE Jan. 1974



$$\text{For Moon; Full range} = \frac{m_e}{ml} \Delta g_e = \frac{22.39}{133.84} \times 8016.61 = 1341.093 \text{ mgal} = 0.3944 \text{ mgal/rev.}$$

$$1 \text{ gross slew} = 103.9 \text{ revolutions} \\ = 40.98 \text{ mgal/gross slew}$$

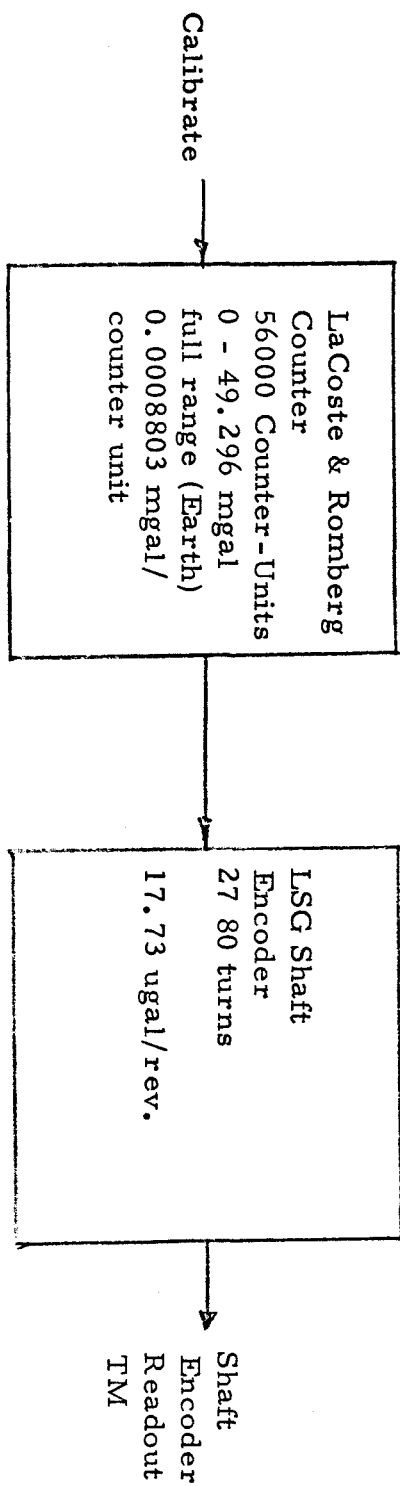
$$1 \text{ vernier slew} = 0.820 \text{ revolutions} \\ = 0.3234 \text{ mgal/vernier slew}$$



## LSCG Sensitivity Calculations

### Appendix B

ASTIR -	PEN. NO.
TM-37	
PAGE	B-2
DATE	Jan. 1974



$$\text{For Moon; Full range} = \frac{m_e}{ml} \Delta g_e = \frac{22.39}{133.84} \times 49.296 = 8.247 \text{ mgal} = 2.966 \text{ ugal/rev.}$$

$$1 \text{ gross slew} = 103.9 \text{ revolutions}$$

$$= 308.2 \text{ ugal/gross slew}$$

$$1 \text{ vernier slew} = 0.82 \text{ revolutions}$$

$$= 2.432 \text{ ugal/vernier slew}$$



**ospace  
ystems Division**

## LSG Sensitivity Calculations

### Appendix B

NO.  
ASTIR-  
TM-37

PAGE B - 3 OF

DATE Jan.

1. c. g. motion of LSG Beam = 0.0042 inches (original adjustment)  
= 0.01067 cm

2. From last preflight PIA test (ref. TP 2365520 p 70 7/27/72) at a Post Amp Gain of 12:

$$\text{Lower Stop Digital Display (Seismic)} \\ = 1,524_8 = 852_{10} \times 19.5 \text{ mv/bit} = 16.614V (-6.614V)$$

$$\text{Upper Stop Digital Display (Seismic)} \\ = 0340_8 = 224_{10} \times 19.5 \text{ mv/bit} = 4.368V (+5.632V)$$

Where 19.5 mv/bit is conversion factor of  
LSG Analog to digital converter

Stop to Stop volts = 12.246 volts = 0.01160 cm  
at Post Amp Gain of 12

Stop to Stop volts =  $\frac{90}{12} \times 12.246 = 91.85$  volts  
at Post Amp Gain of 90 (15th step)

3. c.g. motion of LSG Beam modified by stop movement during vibration testing:

#### Post Vibration Stop Data

$$\text{Lower Stop} = 6.61 \text{ volts} \\ \text{Upper Stop} = 5.63 \text{ volts}$$

$$\text{Shift of Lower Stop} = \frac{6.61}{5.63} \times .0021$$

$$= 0.002466$$

$$\text{New c.g motion} = 0.004566 \text{ in} = 0.01160 \text{ cm}$$

4. Voltage Sensitivity of LSG at Post Amp Gain of 90

$$1 \text{ volt} = 1.263 \times 10^{-4} \text{ cm}$$

$$\text{or } \omega^2 = \Delta g / \Delta x \text{ where } g = \text{gals}, x = \text{cm} \\ \text{or } \omega^2 = 7.918 \text{ ugal/cm/mv}$$



**rospace**  
**Systems Division**

### LSG Sensitivity Calculations

#### Appendix B

NO.  
ASTIR-  
TM-37

PAGE B-4 OF

DATE Jan. 19

#### LSG Data Log

Day 269	Time GMT	Funct.	Seismic Readout Volts	Tide ugal	Remarks
	135000		0.4895		
	135010	Decoder ON			
	142115		-0.1986		
	142212	PA to 15th Step			
	142301		0.1003		
	142604		0.0808		
	142729		0.1003		
	142747	Coarse Screw ON			
	142801		0.0808		
	143013	Vernier dw			
	143054		0.0614		
	143132		0.0808		
	143815	Vernier dw			
	143902		0.0614		
	144225	Vernier dw			
	144300		0.0225		
	144317		0.0419		
	144353		0.0614		
	144402		0.0614		
	144442		0.0419		
	144810	Vernier dw	0.0808		
	144853				
	144934		0.0419		
	144947		0.0419		
	145055		0.0614		
	145102		0.0419		
	145153		0.0419		
	145202		0.0614		
	145217	Bias Out			
	145517		0.0614		
	145526		0.0614		
	145542	Vernier dw			
	145610		0.0614		
	150510	Integ Norm			
	150546		0.0225		
	150622		0.0614		



## LSG Sensitivity Calculations

## Appendix B

NO. ASTIR - TM-37	REV. NO.
PAGE <u>B-5</u>	OF _____
DATE	Jan. 1974

LSG Data Log

D 269	GMT	Funct.	Seismic Readout Volts	Tide ugal	Remarks
150944			0.0614		
151005		Verner down			
151038			0.0030		
151056			0.0225		
151108			0.0030		
151720		Vernier down			
154055		Shaft Eng.Rd			
155244			0.0030		
155421			0.0030		Coarse Screw
155607			-0.0165		3 Vern. Slew; f=1.83 Hz
155614			-0.0165		
155637		Fine Screw On			
155655			0.0030		
155652			0.0030		
155929		Gross Up			
155946			-0.0748		
155957			-0.0554		
160020			-0.1138		
160034			-0.0748		
160125			-0.0748		
160216			-0.0748		
160226			-0.0943		
160443			-0.0943		
161022			0.0748		
161107			-0.0748		
162100			-0.1138		
162358			-0.1138		
162451		Gross Dw			
162534			-0.1138		
162630			-0.0943		
162635			-0.1332		
162706			-0.1916		
162706			-0.1721		
162706			-0.1527		
162706			-0.1527		
162705			-0.1332		
163722			-0.1332		
					Fine Screw
					1 gross up V = -111mv=?

LSG Sensitivity Calculations

Appendix B

NO.	REV. NO.
ASTIR - TM-37	
B-6	
PAGE _____	OF _____
DATE Jan. 1974	

LSG Data Log

1269 P GMT	Funct.	Seismic Readout Volts	Tide ugal	Remarks
163742	Fine Screw On			
163840		-0.1332		
163900	Gross Up			
163926		-0.1332		
163934		-0.1721		
163943		-0.1721		
164010		-0.1721		
164020		-0.1138		
164028		-0.1138		
164040		-0.0943		
164046		-0.1332		
164053		-0.1527		
164101		-0.1138		
164125		-0.1332		
164137		-0.1138		
164143		-0.1916		
164152		-0.1721		
164203		-0.1527		
164406		-0.1138		Fine Screw
164801		-0.1332		1 gross up,no △ V
164825	Gross Up			
164847		-0.1332		
165303		-0.1721		
165347		-0.1332		
165405		-0.1332		Fine Screw
165434		-0.1132		1 gross up; f = 1.78 Hz
165734	SE Readout			C = 3366.5
166146		-0.1132		F = 2570.69
171440		-0.1132		
171535	Coarse Screw On			
171552		-0.1132		
171730	Vernier Up			
171739		-0.1132		
171900	Vernier Up			
171935		-0.0943		
172000	Vernier Up			



## LSG Sensitivity Calculations

## Appendix B

NO.  
ASTIR-  
TM-37

REV. NO.

B-7  
PAGE \_\_\_\_ OF \_\_\_\_

DATE Jan. 1974

LSG Data Log

269 e GMT	Funct.	Seismic Readout Volts	Tide ugal	Remarks
172213	Vernier Up	-0.0748		
172243		-0.0748		
122630				C = 3363.3
173038		-0.0943		
173132	Vernier Up			
173222		-0.0748		
173344		-0.0748		
173400	Vernier Up			
173504		-0.0554		
173520	Vernier Up			
173624		-0.0165		Coarse Screw
173700	Vernier Up			8 Vernier Up; f = 2.12 Hz
1735		0.0030		
26		-0.0165		
174607	SE Readout			C = 3359.2
180648		0.0030		
183036		-0.0165		
183225	Gross Up			
183242		0.0030		
183305		0.1587		
183314		0.1976		
183325		0.2560		
183350		0.3533		
183359		0.4311		
183406		0.4506		
183415		0.4845		
183422		0.5090		
183434		0.5673		
43		0.6452		
451		0.6646		
183516		0.7814		
183533		0.8787		
183544		0.9565		
183539		1.0149		
614		1.1122		
02		1.3652		
183706	Coarse Screw On			
183711		1.3847		

LSG Sensitivity Calculations

Appendix B

NO.	ASTIR-	REV. NO.
	TM-37	
PAGE	B-8	OF
DATE	Jan. 1974	

LSG Data Log

Time GMT	Funct.	Seismic Readout Volts	Tide ugal	Remarks
183732		1.4041		
183835		1.7669		Coarse Screw
184015	Gross Dw			91% Gross Up; f = 2.06 Hz
184050		1.3263		
184134		1.0928		
184223		0.8592		
184300		0.6257		
184423		0.2754		
184439		0.1781		
184454		0.1003		
184509		0.0030		
184518		-0.0359		
184527		-0.0748		
184540		-0.1721		
184607		-0.1527		
185114	Seismic Hi Gain			
185154		0.2365		
185212	Integrate Normal			
185244		0.6646		
185301	Bias In			
185353		0.7230		
185418		0.6646		
185426		1.0344		
185553	Bias Out			
185707		-0.7559		
185720	Seismic Low Gain			
185818		-0.0943		
185827		-0.1138		
185900	Bias In			
185937		-0.943		
190655	Bias Out			Coarse Screw
190845		-0.1138		Gross down; f = 2.07 Hz
190900	Vernier Up			
190944		-0.1138		
191010	Vernier Up			
191030	Vernier Up			
191300	Vernier Up			
191400	Vernier Up			
191444	Vernier Up			



**ospace**  
**ystems Division**

### LSG Sensitivity Calculations

#### Appendix B

ASTIR-  
TM-37

B-9

PAGE \_\_\_\_\_ OF \_\_\_\_\_

DATE Jan. 19

#### LSG Data Log

Day 269	Time GMT	Funct.	Seismic Readout Volts	Tide ugal	Remarks
191525		Vernier Up			
191600		Vernier Up			
191635		Vernier Up			
191713			-0.0359		
191725		Vernier Up			
191758			-0.0165		
191810		Vernier Up			
191908		Vernier Up			
192306			0.0225		
192414			0.0030		
192515		Vernier Up			Coarse Screw 13 Vernier Slew Up; f = 2.19 Hz
192617			0.0614		
193010			0.0614		
193059			0.0225		
193120		Bias In			
194102			0.0614		
194115		SE Readout			C = 3358.06 F = 2570.69
194644			0.0419	57	
201107			0.0419	-47	
201344			0.0419	-59	
201921			0.0415	-81	
201928			0.0419	-81	
202001			0.0419	-83	
202536			0.0419	-105	
205104			0.0419	-201	
205351			0.0419	-213	
205610			0.0419	-220	
205756			0.0419	-227	
210011			0.0419	-235	
210523			0.0419	-254	
210557			0.0419	-256	
210610			0.0419	-256	
210625		Coarse Screw In			
210740			0.0419	-261	
210755		Vernier Dw			
210845			0.0225	-264	



## LSG Sensitivity Calculations

## Appendix B

NO. RE  
ASTIR-  
TM-37  
B-10  
PAGE \_\_\_\_ OF  
DATE Jan. 19

LSG Data Log

Day 269		Seismic Readout	Tide	
Time GMT	Funct.	Volts	ugal	Remarks
210935	Vernier Dw	0.0225	-266	
211016		0.0225	-266	
211028		0.0225	-271	
211505		0.0225	-271	
211611		0.0225	-271	
211625	Coarse Screw Off	0.0225	-271	
211639		0.0030	-275	
211952		0.0030	-275	
212102		0.0030	-275	
212010	SE Readout			C = 3359.68 F = 2520.7
212452		-0.0165	-275	
212628		0.0030	-280	
212704		-0.0165	-280	
212818		-0.0165	-281	
213026		0.0030	-283	
213202		0.0030	-283	
213252		-0.0165	-285	
213342		0.0030	-285	
213433		-0.0165	-285	
213522		0.0030	-287	
213613		0.0030	-287	
213653		-0.0165	-287	
213743		0.0030	-288	
213844		0.0030	-288	
213943		0.0030	-290	
214010	Seis Hi Gain			
214044		-1.3397	-290	
214144		-0.0359	-290	
214244		0.6841	-292	
214344		0.0030	-292	
214845		-0.6392	-292	
215427		-0.5029	-299	
215810	Decoder Off			
215846		0.2365	-302	
220328		-0.6781	-305	

Appendix A

LSG Transfer Functions\*

NO.  
ASTIR-  
TM-37

REV. NO.

PAGE \_\_\_\_\_ OF \_\_\_\_\_

DATE

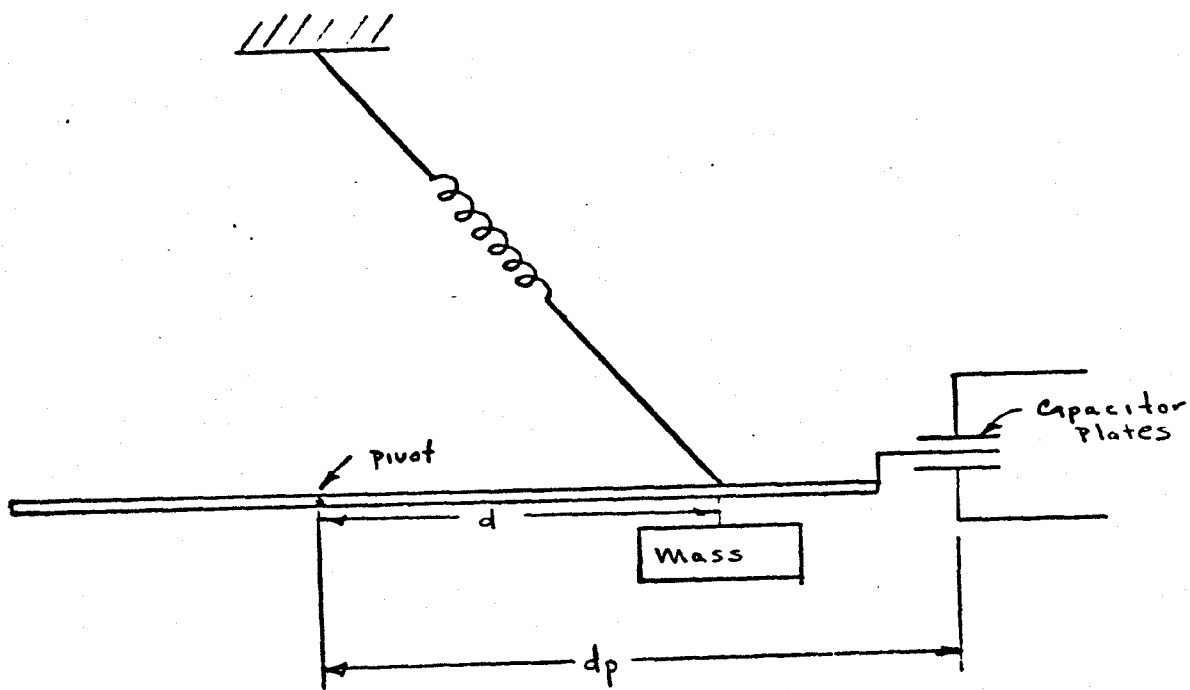


Figure 1 LSG Sensor

Equation of Motion

$$(1) I \ddot{\delta} + 2 I \xi \omega_0 \dot{\delta} + I \omega_0^2 \delta = md \Delta g - dp F_e$$

which may be simplified to

$$(2) \ddot{x} + 2 \xi \omega_0 \dot{x} + \omega_0^2 x = \left(\frac{d}{dg}\right)^2 \Delta g - \left(\frac{d}{dg}\right)^2 \left(\frac{dp}{d}\right) \frac{F_e}{m}$$

where  $I = mdg^2$  and  $dg =$  radius of gyration around pivot.

$d$  = distance from pivot to c.g.

$F_e$  = capacitor plate electrical feed back force

---

\* Reference BxA Memo 984-683 of 19 May 1972 by M. Dela Cruz, entitled "Flight LSG Characteristics"

## Appendix A

## LSG Transfer Functions

NO.  
ASTIR-  
TM-37

REV. NO.

PAGE 1 OF 1

DATE

 $x$  = c.g. vertical motion $\omega_0$  = natural frequency of sensor $m$  = total sensor mass

The electrical force on the beam is:

$$(3) \quad F_e = \frac{2 C_o V_o}{d_o} V_f - \frac{C_o}{d_o^2} \left[ (1 - k_s \cos \phi) V_c^2 + 2 V_o^2 + V_f^2 \right] x$$

where  $C_o = 3.5 \times 10^{-12}$  farads, the center plate to fixed plate capacitance $d_o = .515 \times 10^{-1}$  cm, the center plate to fixed plate spacing $V_o = 6.5V$ , the dc bias voltage plate to ground $V_f = 0$  to  $5.5V$  (approximately), the feed back voltage $k_s \approx \frac{2 C_o}{C_s + 2 C_o}$ , where  $k_s$  is the capacitance bridge constant $C_s \approx 27.30 \times 10^{-12}$  farads, the stray capacitance of the sensor to preamp input including cable capacitance $\phi = \tan^{-1} B/A$ , the bridge circuit phase angle $B = \frac{1 - \alpha^2}{2 R_L C_o W_c}, \quad \alpha = \frac{x}{d_o}$  $A = \frac{1 + (1 - \alpha^2)}{2 C_o} C_s$  $R_L = 5$  megohm, the load resistance seen by the bridge circuit $W_c = 2\pi f_c$ , where the carrier frequency is  $3.3$  kHz $V_c = 0.5V$ , the peak value of the carrier signal

From equation (2) and (3), the X terms may be combined to provide

## Appendix A

## LSG Transfer Functions

NO.  
ASTIR-  
TM-37

REV. NO.

PAGE 3 OF \_\_\_\_\_

DATE

$$(4) \ddot{x} + 2\xi\omega_0 \dot{x} + \left\{ \omega_0^2 - \left( \frac{d}{dg} \right)^2 \left( \frac{dp}{d} \right) \left( \frac{1}{m} \right) \frac{C_o}{d^2} \right\} \left[ (1 - ks \cos \phi) V_c^2 + 2V_o^2 + V_f^2 \right] x \\ = \left( \frac{d}{dg} \right)^2 \Delta g - \left( \frac{d}{dg} \right)^2 \left( \frac{dp}{d} \right) \left( \frac{1}{m} \right) \left( \frac{2 C_o V_o}{d_o} \right) V_f$$

Equation (4) is the system dynamics equation for closed loop operation. The block diagram for the system is shown in Figure 2, where the  $\omega_{oc}$  term is the period of the sensor modified by the feedback electrostatic force shown in (4). In the closed loop configuration the two switches are thrown in the direction indicated. For open loop operation the switches are switched to the opposite direction and, since no electrostatic feedback force is present, the sensor transfer function becomes

$$(5) \frac{1}{s^2 + 2\xi\omega_0 s + \omega_0^2}$$

where  $\omega_0$  is the natural period of the sensor and  $\xi$  the damping factor.

Referring to Figure 2 the constants and transfer functions are:

$K_b = 88.4$  volts/cm, where  $K_b$  is the capacitance bridge transfer function and 88.4 V/cm is the measured value for the flight LSG.

Post Amp = 1-90, where the post amplifier gain may be stepped in 15 increments of 6 i.e. the 8th step is a gain of 48 (47.5 measured for flight).

Demodulator = 0.636, for the LSG demodulator transfer function

integrator =  $\frac{0.019}{s}$  for the ideal case and is

$$\frac{0.019}{s + 9.2 \times 10^{-6}} \text{ for the flight model}$$

where  $9.2 \times 10^{-6}$  is due to leakage and is the worst case value equivalent to 25 millivolts leakage in 5 minutes at 9 volts.

## Appendix A

## LSG Transfer Functions

NO.  
ASTIR-  
TM-37

REV. NO.

PAGE 4 OF \_\_\_\_\_

DATE

$$\left(\frac{d}{dg}\right)^2 \left(\frac{2 C_0 V_0}{d o m}\right) \frac{dp}{d} = 9.2 \times 10^{-5} \frac{\text{cm}}{\text{sec}^2 \cdot \text{volt}}$$

is the feedback

factor, where the constants are as defined above and

$d$  = 3.06 cm and is the distance from pivot to c. g.

$dp$  = 4.53 cm and is the distance from pivot to the center of the capacitor plates

$dg$  = 1.03  $d$ , and is the radius of gyration

$m$  = .13375 kgm and is the flight sensor mass

There are four sensor cases which response curves are to be developed and they are:

- 1) Flight design open loop where the period of the sensor is 20.7 sec (lunar period), the damping factor is 0.755 (lunar)
- 2) Flight design closed loop where the period and damping factor are as 1) above but the transfer function is modified by the electrostatic feedback force
- 3) Flight sensor in the present configuration open loop where the period is 0.5 seconds and the Q of the sensor is 25.
- 4) Flight sensor in the present configuration closed loop where the period and Q of the sensor are as 3) above.

The transfer function for the four cases are

$$1) \quad \frac{1}{s^2 + 0.458 s + .0919}$$

$$2) \quad \frac{1}{s^2 + 0.458 s + .0719}$$

$$3) \quad \frac{1}{s^2 + 0.502 s + 158}$$

Appendix A

LSG Transfer Functions

NO.  
ASTIR-  
TM-37

REV. NO.

PAGE 5 OF \_\_\_\_\_

DATE

4)

$$\frac{1}{s^2 + 0.502 s + 157.98}$$

Referring to Figure 2, the free modes output is amplified and filtered by an amplifier with the following characteristics:

Gain **498**

2-pole high pass **.00083 Hz**

butterworth filter

Phase lag filter **0.14 Hz and 70 Hz**

the transfer functions for this element of the system is

$$\frac{1.9 \times 10^5 s^2}{(s^2 + 7.35 \times 10^{-3} s + 2.71 \times 10^{-5})(s + .88)(s + 440)}$$

Combining the filter transfer function with the appropriate open and closed loop sensor configuration described above and the remaining elements of the system shown in Figure 2, the transfer functions for the four cases are:

1)

$$\frac{7.68 \times 10^8 s^2}{s^6 + 441.4 s^5 + 592.3 s^4 + 222.3 s^3 + 37.17 s^2 - .266 s + .000962}$$

2)

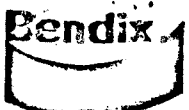
$$\frac{9.76 \times 10^6 s^2}{s^7 + 441.4 s^6 + 604.3 s^5 + 220.8 s^4 + 31.72 s^3 + 2.04 s^2 + .0141 s + .000049}$$

3)

$$\frac{7.68 \times 10^8 s^2}{s^6 + 440.9 s^5 + 769.7 s^4 + 69,6985 s^3 + 61,700 s^2 + 450 s + 1.65}$$

4)

$$\frac{9.76 \times 10^6 s^2}{s^7 + 441.4 s^6 + 769.7 s^5 + 69,769 s^4 + 61,703 s^3 + 451.8 s^2 + 1.668 s + .000049}$$



Aerospace  
Systems Division

## Appendix A

### LSG Transfer Functions

NO. ASTIR-	REV. NO.
TM-37	
PAGE <u>6</u>	OF <u>  </u>
DATE	

Where the output of the functions are in units of volts/gal and the value of post amp gain was 47.5 (8th step). Figures 3 and 4 are plots of the response curves using the above functions. Figure 4 shows the response to the LSG if the period of sensor could be increased to 1 sec where the damping was assumed constant ( $Q = 12.5$ ).

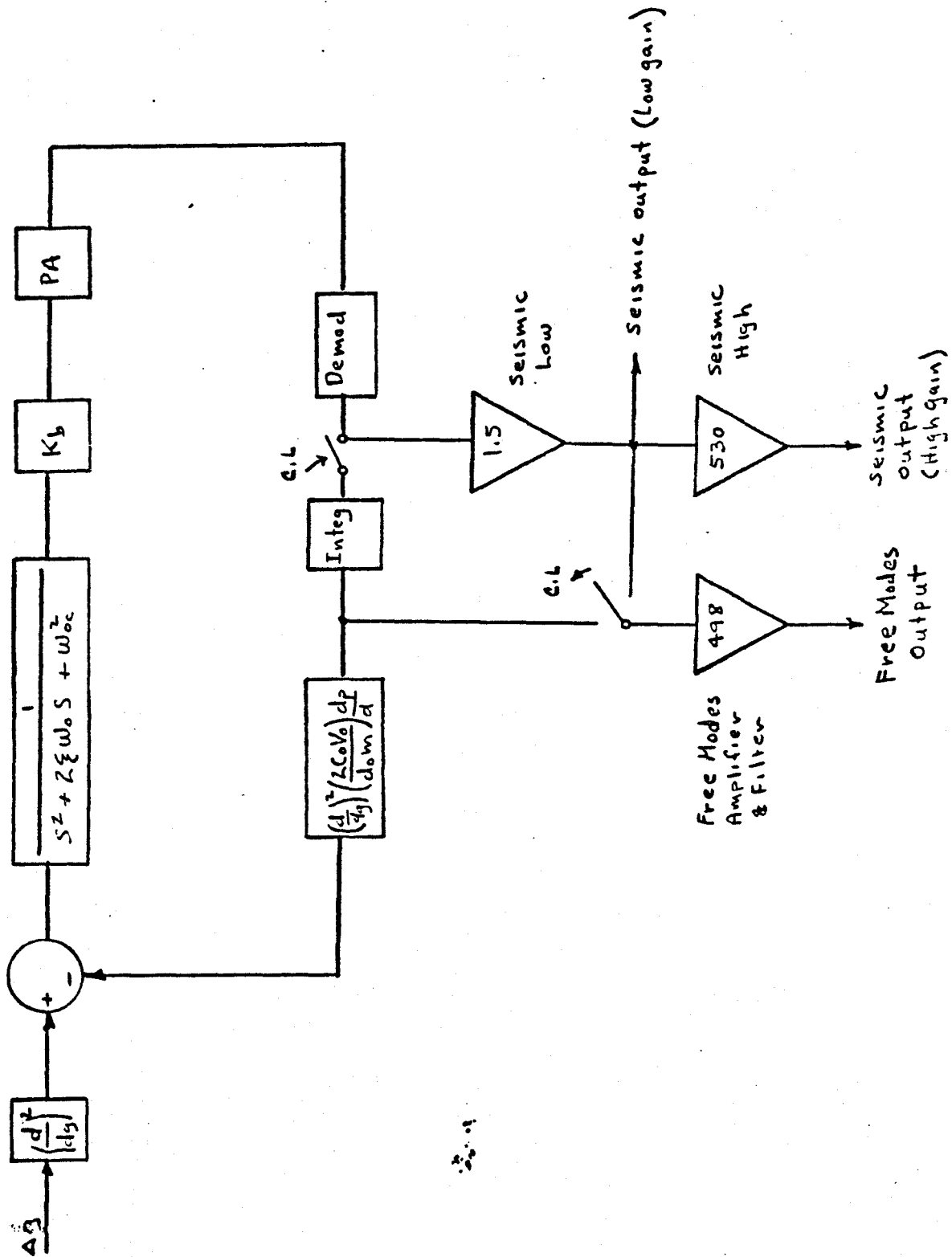


Figure 2

MODEL

DATE

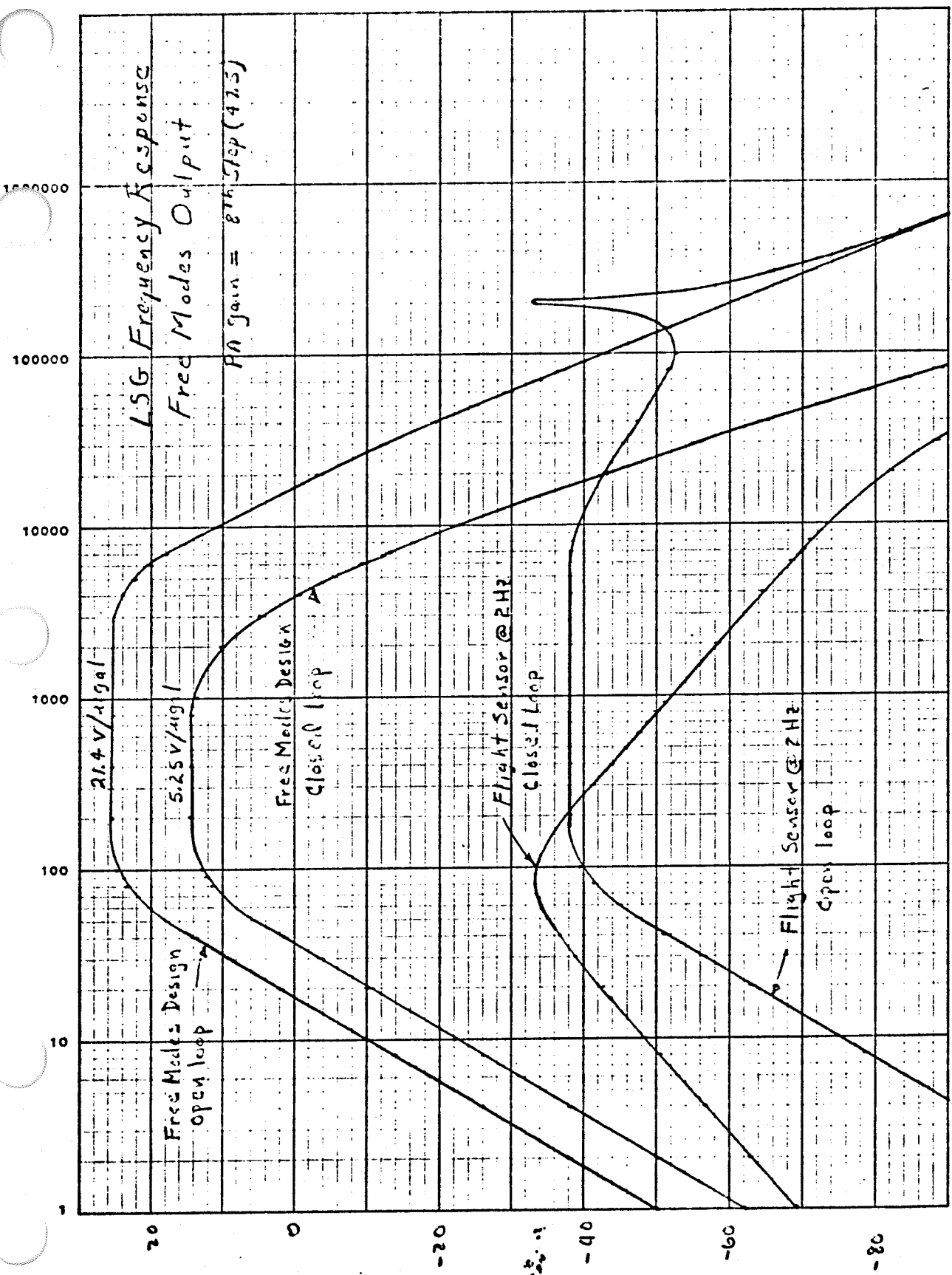


Fig. 3

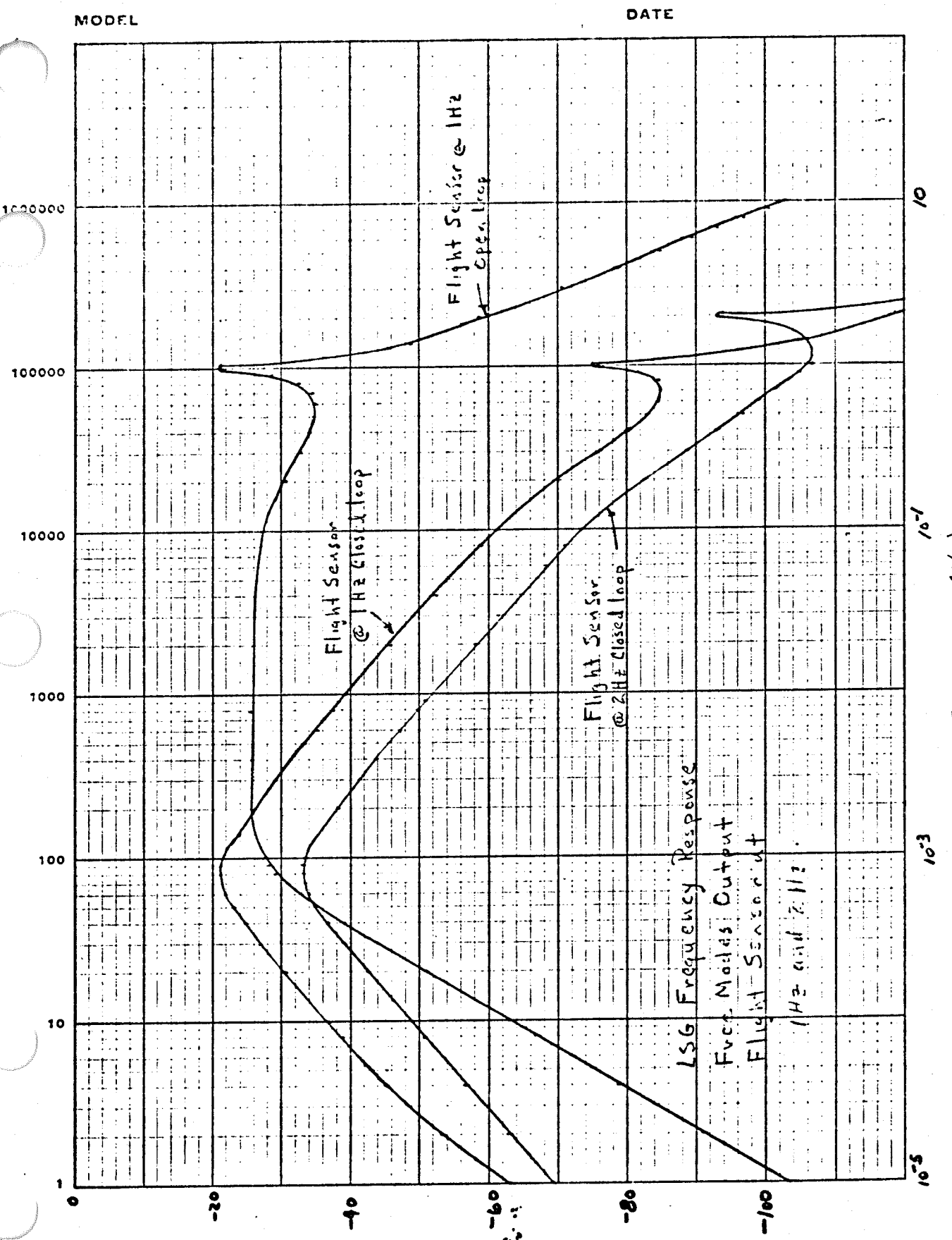
Frequency (Hz)

10

10<sup>-1</sup>10<sup>-3</sup>10<sup>-5</sup>

(125m/V) 1-Freq Selection of Compensation

Fig. 4



dB relative to V0115/avg1 (V0115/avg1)